

# TIME-RESOLVED *HST* SPECTROSCOPY OF FOUR ECLIPSING MAGNETIC CATAclysmic VARIABLES<sup>1,2</sup>

GARY D. SCHMIDT

Steward Observatory, The University of Arizona, Tucson, AZ 85721

AND

H.S. STOCKMAN

Space Telescope Science Institute, 3700 San Martin Dr., Baltimore, MD 21218

*Accepted for publication in the Astrophysical Journal*

## ABSTRACT

Time-resolved, multi-epoch, *Hubble Space Telescope* ultraviolet eclipse spectrophotometry is presented for the magnetic cataclysmic variables (mCVs) V1309 Ori, MN Hya, V2301 Oph, and V1432 Aql. Separation of the eclipse light curves into specific wavebands allows the multiple emission components to be distinguished. Accretion-heated photospheric spots are detected in V1309 Ori and V2301 Oph, indicating covering factors  $f < 0.015$  and  $\sim 0.008$ , and blackbody temperatures  $T_{\text{spot}} > 150,000$  K and  $\sim 90,000$  K, respectively. The cyclotron-emitting shock on MN Hya is detected in the optical/near-UV and found to occupy no more than  $f = 0.004$  of the stellar surface. Emission from the accretion stream is a prominent component in V1309 Ori and V2301 Oph, and the protracted eclipse ingress of UV emission lines in the latter object indicates that the stream penetrates the white dwarf magnetosphere to a height of  $\sim 9 R_{\text{wd}}$  before it is funneled onto the magnetic poles. The UV emission-line spectrum of V1309 Ori (and to a lesser extent, MN Hya) is unusual among mCVs, with the relative strength of N V  $\lambda 1240$  in V1309 Ori matched only by the asynchronous system BY Cam. The prominence of N IV  $\lambda 1718$  suggests that an overabundance of nitrogen may be the most likely explanation.

Three epochs of observation of the asynchronous V1432 Aql cover about one-third of a 50-day lap cycle between the white dwarf spin and binary orbit. The eclipse light curves vary enormously from epoch to epoch and as a function of waveband. The dereddened UV spectrum is extremely bright compared with the optical, and the overall spectral energy distribution coupled with the duration of eclipse ingress indicate that the dominant source of energy is a hot ( $T_{\text{wd}} \sim 35,000$  K) white dwarf. This explanation also accounts for the modest brightness variation out of eclipse and the weakness of optical circular polarization due to cyclotron emission. Undiminished line emission through eclipse indicates that the eclipse itself is caused by a dense portion of the accretion stream, not the secondary star. The temperature of the white dwarf in V1432 Aql greatly exceeds that in any other AM Her system except the recent nova V1500 Cyg. This, combined with its current asynchronous nature and rapid timescale for relocking, suggests that V1432 Aql underwent a nova eruption in the past  $\sim 75 - 150$  yr. The reversed sense of asynchronism, with the primary star currently *spinning up* toward synchronism, is not necessarily at odds with this scenario, if the rotation of the magnetic white dwarf can couple effectively to the ejecta during the dense wind phase of the eruption.

*Subject headings:* binaries: eclipsing — stars: magnetic fields — novae, cataclysmic variables — stars: individual (V1309 Ori, MN Hya, V2301 Oph, V1432 Aql)

## 1. INTRODUCTION

At least 11 of the nearly 5 dozen known AM Her variables are true eclipsing binaries where light curves through eclipse can be used to analyze the structure and relative importance of emission regions on the magnetic white dwarf and in the accretion column that connects it to the mass-losing companion. The eclipsing systems are found with magnetic field strengths  $7 < B < 60$  MG (MG =  $10^6$  G), span the orbital period range  $1.5 < P_{\text{orb}} < 8.0$  hr, and include one asynchronous system. Thus, there is reasonable assurance that an understanding gained from the eclipsing systems can be applied to the class as a whole

(see Cropper 1990 for a general review).

Because the magnetic field funnels accreting gas onto impact regions as small as  $f = A_{\text{spot}}/4\pi R_{\text{wd}}^2 \sim 10^{-3}$ , high time resolution,  $\Delta t \lesssim 1$  s, plus an adequate photon rate are required to resolve the structures. The wavelength region of choice is the ultraviolet, where the white dwarf and heated impact region are prominent ( $T_{\text{wd}} \sim 15,000$  K and  $T_{\text{spot}} \gtrsim 30,000$  K, respectively), line and continuum emission from the funnel gas is available, and the contribution from the late-type secondary star is minimized. The first two papers in this series presented *HST* time-resolved spectroscopy of DP Leo (Stockman et al. 1994, hereafter

<sup>1</sup>Based on observations with the NASA/ESA *Hubble Space Telescope* obtained at the Space Telescope Science Institute, which is operated by the Association of Universities for Research in Astronomy, Inc., under contract NAS 5-26555.

<sup>2</sup>Some ground-based observations reported here were obtained at the Multiple Mirror Telescope Observatory, a facility operated jointly by the Smithsonian Institution and the University of Arizona.

Paper I) and UZ For (Stockman & Schmidt 1996, hereafter Paper II); the latter study also applied the method to ST LMi, where the accretion footpoint undergoes “self-eclipse” when it rotates behind the white dwarf limb. DP Leo was observed in a state of very low accretion, nevertheless the eclipse light curves revealed the contribution of an accretion-heated spot ( $T_{\text{spot}} \sim 50,000$  K) against the surrounding white dwarf photosphere ( $T_{\text{wd}} \sim 16,000$  K). The fractional surface area of the near-UV spot,  $f \sim 0.006$ , was found to be very similar to that of the optical cyclotron source in a high state. Observations of UZ For showed that the accretion stream itself can be a dominant UV source in an active accretion state, owing to both strong resonance line emission and free-bound continua. The temperature of the hot spot was measured at  $T \gtrsim 30,000$  K and found to occupy at least  $f = 0.01$  of the white dwarf surface area. Attempts to model the line emission led to a two-phase composition for the gas stream, consisting of low filling-factor, dense clumps threading a more rarefied flow. Many of the observed properties of UZ For in the UV are shared by the well-studied HU Aqr (e.g., Schwobe 1998), and similar conclusions have been reached.

In this paper we present Faint Object Spectrograph (FOS) spectroscopy of the final 4 eclipsing magnetic cataclysmic variables (mCVs) observed in this program. All four are relatively bright when actively accreting,  $V < 17$ , and together display an interesting variety of properties: V1309 Ori is the longest-period AM Her system known, with an eclipse persisting for more than 40 min. Given the rather modest magnetic field of  $B \sim 60$  MG, spin-orbit locking in this binary challenges current theories of the magnetic interaction mechanism. In the high state, MN Hya is a classic 2-pole accretion system whose strong optical polarization enables detailed models. The weakest magnetic field measured on any AM Her system is found on V2301 Oph, a characteristic which has frustrated polarimetrists but motivated a number of photometric and spectroscopic analyses. V1432 Aql is the only one of the 4 for which an eclipse by the secondary star is in doubt; it is also the sole asynchronous eclipsing system, made all the more unusual because the spin period appears to *exceed* the orbital period by 0.3%. These and other properties of the systems are summarized together with basic references to previous work in Table 1.

Recently, several sophisticated techniques used to study the emission of disk CVs have found their way to magnetic systems. These include Doppler tomography (e.g., Schwobe et al. 1999) and maximum entropy methods (MEM) for modeling eclipse light curves in broad bands (Harrop-Allin, Hakala, & Cropper 1999b; Harrop-Allin et al. 1999a) as well as of full-orbit phase-resolved emission-line spectroscopy (Sohl & Wynn 1999; Vrielmann & Schwobe 1999; Kube, Gänsicke, & Beuermann 2000). Several of these approaches utilize Genetic Algorithms (e.g., Hakala 1995) to efficiently approach global optimization of the many model variables.

Each of the methods has its strengths and limitations. Doppler tomography maps the velocity distribution of emitting regions, not their locations, and the technique is insensitive to motions out of the orbital plane (see, e.g., Schwobe et al. 1999). MEM and genetic optimization codes were developed in an attempt to deal with

the tremendous ambiguity of generalized model-fitting approaches, where the number of emitting sources may exceed the number of independent data points. The various tools are in many ways complementary and together represent the state-of-the-art in analytical techniques for time-resolved studies of accretion binaries.

We have chosen to apply a more qualitative approach to interpret the eclipse light curves of these mCVs for several reasons. First, the photon rate in the near-UV from *HST*+FOS cannot compete with what is now commonplace from modern instrumentation and large ground-based telescopes working in the visible ( $\sim 0.35 - 1.0 \mu\text{m}$ ). This, plus the low spectral resolution of FOS effectively rule out quantitative Doppler studies of the emission lines. Time allocation considerations on *HST* limited the observing program on each source to windows just encompassing eclipse, and for some targets scheduling constraints precluded obtaining both ingress and egress at the same epoch. With such limitations, the data presented here are amenable to identifying the location and relative importance of principle sources of line and continuum emission, but not for unraveling their detailed structure or kinematics.

## 2. OBSERVATIONS

Time-resolved UV spectra of V1309 Ori, MN Hya, V2301 Oph, and V1432 Aql were obtained with *HST* at several epochs between 1996 Aug. 3 and 1996 Dec. 24 (Cycle 6, post-COSTAR), as recorded in Table 2. Setup of the FOS was as follows: the G160L grating and  $0.86''$  square C-1 aperture pair to provide a spectral coverage of  $\lambda\lambda 1180 - 2500$ ,  $2\times$  substepping for a resolution of  $\sim 7 \text{ \AA}$ ; RAPID readout mode with a time resolution of 0.8201 s per spectrum; and  $5\times$  overstepping to eliminate gaps caused by dead diodes. Data calibration was carried out as in Papers I and II, using the *calfos* reduction pipeline. Observations of V1309 Ori and V1432 Aql were obtained at several epochs each: the former to adequately cover the long eclipse and the latter to sample the range of eclipse behavior shown by this asynchronous system. The eclipse interval of V2301 Oph was missed in the initial observation due to a spacecraft scheduling error, and the object was revisited a month later. Even then, egress was not adequately covered. MN Hya was found in a very faint state in the first pointing but had brightened by an order of magnitude upon a second visit 70 days later.

The low accretion state of MN Hya in mid-Oct. 1996 was confirmed by a contemporaneous ground-based spectrum that showed a visual magnitude  $V > 20$  and no obvious emission lines. This and a number of other supporting optical observations were obtained over the time period of the spacecraft observations. In the cases of V1309 Ori, MN Hya, and V2301 Oph, the Blue Channel spectrograph of the MMT provided flux-calibrated spectra covering the range  $\lambda\lambda 3300 - 6700$ . In addition, a full orbital cycle of unfiltered photometry and circular polarimetry with a time resolution of  $\sim 45$  s was acquired during an active phase of MN Hya on 1996 Jan. 27 (9 months prior to the initial *HST* visit) with the Octopole polarimeter attached to the 2.3 m Bok telescope of Steward Observatory. A 3500 – 6500 Å eclipse light curve of the same object with 128 ms time samples was obtained on 1996 Mar. 10 using a programmed-readout mode of the CCD in the MMT

Red Channel spectrograph (Schmidt, Weymann, & Foltz 1989). For this observation, the disperser was replaced by a plane mirror and both the target and a nearby comparison star were located in the spectrograph slit. The light curve of the latter object enabled a quality eclipse profile of MN Hya despite the presence of light clouds. Finally, occasional spectra and circular spectropolarimetry spanning  $\sim \lambda\lambda 4000 - 8000$  were obtained with the CCD Spectropolarimeter (Schmidt, Stockman, & Smith 1992) attached to the Steward Observatory 2.3 m telescope. The ground-based observations are also summarized in Table 2.

### 3. RESULTS

#### 3.1. *Interpreting the UV Light Curves*

Light curves were prepared from the time-resolved UV spectroscopy in 4 wavelength bandpasses in a manner similar to the procedure described in Papers I and II. The wavebands extracted from the dispersed spectrum are: a near-UV interval (NUV;  $\lambda\lambda 1895 - 2505$ ); the far-UV continuum (FUV;  $\lambda\lambda 1254 - 1522$  excluding Si IV  $\lambda 1397$ ); and the emission lines C IV  $\lambda\lambda 1548, 1551 +$  He II  $\lambda 1640$ , constructed by summing a pair of continuum-subtracted bands covering  $1529 - 1568 \text{ \AA}$  and  $1623 - 1655 \text{ \AA}$ . In addition, a “white-light” curve was derived from the zero-order undispersed image. This bandpass has an effective width of  $\sim 1900 \text{ \AA}$  for these sources and central wavelength of  $\sim 3400 \text{ \AA}$ . The light curves for V1309 Ori, MN Hya, V2301 Oph, and V1432 Aql are shown as montages plotted vs. orbital phase in Figures 1 – 4, respectively. An approximate absolute calibration of the 3 UV channels in units of flux per detected count per 0.82 s sample is: C IV+He II:  $2.0 \times 10^{-13} \text{ ergs cm}^{-2} \text{ s}^{-1}$ ; FUV:  $9.3 \times 10^{-16} \text{ ergs cm}^{-2} \text{ s}^{-1} \text{ \AA}^{-1}$ ; NUV:  $7.4 \times 10^{-17} \text{ ergs cm}^{-2} \text{ s}^{-1} \text{ \AA}^{-1}$ . Note that the two continuum bands are characterized per unit wavelength. Neither V1309 Ori nor V2301 Oph displayed discernible variations in eclipse shape over the various epochs, in the former despite a span of more than 2 months. For these objects, mean light curves are shown<sup>3</sup>. MN Hya was too faint in the initial visit to provide useful data so only the second data set is displayed. It should be noted that the quoted accuracies of all ephemerides (Table 1) are sufficient to phase the data presented here to an accuracy of  $\sigma_\varphi < 0.004$  for all but V1309 Ori, where the uncertainty is  $\pm 0.008$ .

The mean spectrum of each of the 4 objects as it emerged from the processing pipeline showed evidence for the  $2200 \text{ \AA}$  silicate depression due to interstellar absorption. Using the extinction curve from Cardelli, Clayton, & Mathis (1989) and  $R = A_V/E(B - V) = 3.1$ , corrections were applied to each spectrum with an eye toward producing as smooth a continuum as possible in the region  $\sim 1700 - 2500$ . The results, quoted in Table 1, indicate visual extinctions in the range  $0.1 \leq A_V \leq 0.7 \text{ mag}$ , with uncertainties of  $0.05 - 0.1 \text{ mag}$ .

For typical system parameters, eclipse by the secondary of a point on the white dwarf has a maximum duration of  $\Delta\varphi \sim \pm 0.04$  ( $\sim 10 - 40 \text{ min}$  total length), with a weak dependence on binary period. Eclipse transition across the white dwarf disk itself requires a phase interval  $\Delta\varphi \gtrsim 0.004$  (at least 30 s), with the inequality reflect-

ing the dependence on primary star mass, orbital period (greater for shorter  $P$ ), and inclination (greater for smaller  $i$ ). Previous studies (e.g. UZ For, Paper II) have found that the accretion column is a strong source of not only line emission, but also optical-UV continuum. Because the gas stream approaches the primary in a curved, prograde path (see, e.g., Lubow & Shu 1975) and dynamically couples to the magnetic field en route, covering of the accretion column can commence prior to the white dwarf eclipse and continue long after. Moreover, depending on the colatitude of the impact region on the star, the stream may arc out of the orbital plane and undergo only a partial eclipse. At the accretion shock, optical-IR cyclotron emission typically originates over a region of the stellar surface with  $f_{\text{cyc}} \sim 0.001$ . A somewhat larger portion of the disk  $0.001 \lesssim f_{\text{spot}} \lesssim 0.1$  is heated by low-level accretion or the EUV-bright base of the accretion column to a characteristic temperature  $kT \approx 10 - 30 \text{ eV}$ . For a circular profile, eclipse of this hot spot will produce an abrupt drop in the FUV flux over an interval  $1 \text{ s} \lesssim \Delta t \lesssim 10 \text{ s}$ , depending on the observed waveband. The smallest spots are not resolvable at our sampling frequency (and measured UV count rates).

Therefore, the baseline behavior that we expect through eclipse is: 1) Initially a gradual extinction of the emission-line flux, beginning with the gas stream near the secondary and proceeding along the flow; 2) A brief decline in the white light and NUV continuum bands that is well-resolved at the FOS sampling rate, corresponding to the limb of the secondary beginning to pass over the white dwarf disk; 3) An abrupt, possibly unresolved, drop in the FUV and to a lesser extent, the NUV bands, as the accretion-heated spot on the white dwarf is eclipsed. This transition will very nearly coincide with a similar extinction of the cyclotron flux in the white light channel. Continuing through the light curve, we find 4) The conclusion of the resolved white dwarf eclipse; 5) Continued obscuration of the prograde portion of the gas stream; 6) A period of nearly constant minimum light lasting up to several minutes; and 7) – 11) An egress sequence that is a vertically-mirrored repeat of steps 1) – 5), in order, as each component is progressively exposed. Barring changes in viewing perspective or in the beaming factor of an emission component, amplitudes of corresponding ingress/egress transitions will be identical. The Rosetta Stone for this basic behavior is UZ For (Paper II).

#### 3.2. *V1309 Ori (RX J0515.6+0105)*

V1309 Ori has the longest orbital period of the known AM Her binaries at 7.98 hr. The UV (Figure 5) and optical spectra (Garnavich et al. 1994; Shafter et al. 1995) are dominated by continuum and line emission from the accretion stream. Buckley & Shafter (1995) report the detection of weak, variable circular polarization in a white-light optical bandpass. Spectropolarimetric observations of the system obtained by us in 1994 Nov. (not shown) confirm a low level of polarization for the system ( $|v| \lesssim 2\%$ ) as well as the existence of cyclotron emission harmonics centered near  $\lambda\lambda 4425, 5510, 6625$  in both total flux and polarization. Identifying these with harmonic numbers  $m = 5, 4, 3$ ,

<sup>3</sup>Count rates from the second epoch on V2301 Oph were scaled up by a factor 1.5 prior to averaging to adjust for an apparent reduction in activity over the month-long interval.

respectively, we substantiate previous estimates of the primary magnetic field strength near 61 MG (Garnavich et al. 1994; Shafter et al. 1995; Harrop-Allin et al. 1997). The polarization appears to vary synchronously on the orbital period and is probably strongly diluted by light from the accretion stream. It is remarkable that such a wide binary can maintain synchronism given the implied accretion rate and modest magnetic field (see also Frank, Lasota, & Channugam 1995 and Harrop-Allin et al. 1997). Nevertheless, the 1996 UV light curves shown in Figure 1 are so similar to published visible-light profiles from 1993 – 1997 (e.g. Shafter et al. 1995), and so unlike the variable light curves exhibited by asynchronous systems (e.g., §3.5), that we conclude the spin and orbital motions are indeed locked. Interestingly, V1309 Ori displays an extremely peculiar X-ray behavior (Walter, Scott, & Adams 1995; de Martino et al. 1998), accreting in bursts as short as a few seconds duration whose local  $\dot{m}$  values fall in the domain of buried accretion shocks (Beuermann & Woelk 1996), and which cool primarily in the soft X-rays (e.g., Szkody 1999). This extreme flickering does not appear in the UV light curves recorded by FOS.

The V1309 Ori eclipse light curves shown in Figure 1 and at an expanded scale in Figure 6 confirm the dominance of the accretion stream in the UV. Apart from inflections in the continuum bands at the beginnings of ingress and egress, all four channels display protracted transitions ( $\Delta\varphi = 0.025$ ). The lack of sharp transitions in the white-light continuum places an upper bound on the cyclotron emission in this band ( $\lesssim 5\%$ ). The inflections themselves are of approximately the correct duration ( $\Delta\varphi \sim 0.005$ ) to ascribe to an eclipse of the white dwarf, but this explanation requires a hot photosphere,  $T_{\text{wd}} > 30,000$  K. The interpretation is also complicated by the simultaneous egress of the line-emission region at  $\varphi = 0.035$  as is evidenced by the emission-line channel.

On the other hand, a sharp drop in the FUV channel at  $\varphi = 0.952$  is strong evidence for the presence of an accretion-heated spot on the white dwarf. The data are sufficiently noisy that we show this light curve in Figure 6 after smoothing by a running mean of width 10 samples (8 s). The ingress time for the spot as measured from the two contacts  $c_1$ ,  $c_2$  indicated in the figure is  $6 \pm 2$  s, implying that the transition is unresolved in the smoothed data. We therefore can set only an upper limit to the azimuthal extension of the spot as  $< 2 \times 10^8$  cm. The implied covering factor for a circular spot on a  $0.6 M_{\odot}$  white dwarf is  $f_{\text{spot}} < 0.015$ , possibly larger if the star is over-massive. The reduction in FUV flux corresponding to this drop is  $\sim 2.2$  counts sample $^{-1}$ , or a dereddened flux of  $3.2 \times 10^{-15}$  ergs cm $^{-2}$  s $^{-1}$  Å $^{-1}$  at an effective wavelength of  $\sim 1400$  Å. For a distance  $D > 500$  pc, the corresponding blackbody temperature is  $T_{\text{spot}} > 150,000$  K ( $kT > 13$  eV).

For V1309 Ori, removal of the 2200 Å feature was accomplished with a minor amount of absorption,  $A_V = 0.15 \pm 0.05$  mag, despite a distance of at least 500 pc. The dereddened spectra are shown in Figure 5 and characterized by the line strength measurements compiled in Table 3. Out of eclipse, V1309 Ori shows the high excitation line O V  $\lambda 1370$  as well as extraordinarily strong N V  $\lambda 1240$ . The lines persist weakly through eclipse ( $0.98 < \varphi < 0.02$ ), attesting to a small, continuously-

exposed portion of the funnel or corona on the secondary star. The remarkable strength of N V  $\lambda 1240$  has already been noted by Szkody & Silber (1996) from an *IUE* spectrum. The ratio N V  $\lambda 1240$ /C IV  $\lambda 1549 = 7.2$  is exceeded among known mCVs only by BY Cam at one epoch (Bonnet-Bidaud & Mouchet 1987; Shrader et al. 1988); indeed among mCVs in general this ratio rarely approaches unity. With  $\sim 30$  eV separating the ionization stages, the very large ratio implies at minimum a hot ionizing continuum and high density conditions. However, more detailed analysis by Bonnet-Bidaud & Mouchet found that the line ratios for BY Cam were so extreme that a nitrogen enhancement was indicated. Proposed enrichment mechanisms included accretion from a companion whose hydrogen-rich layers had already been stripped, or mixing of normal stellar material with nuclear-processed matter: either nova ejecta or possibly surface material of the white dwarf. For stripping of an initially main-sequence secondary, the orbital period of V1309 Ori would require that well over a solar mass of material has been shed by the secondary over the lifetime of the binary – a very unlikely scenario. The fact that the N V/Si IV, N V/C IV line ratios place V1309 Ori precisely atop the tight grouping of 4 of the 5 measurements for BY Cam (Bonnet-Bidaud & Mouchet 1987) would seem to argue against a mechanism that involves mixing of unprocessed and processed material – either from a previous nova eruption or from within the secondary star. Nevertheless, a nitrogen abundance anomaly would seem to be the best explanation since N IV  $\lambda 1718$  is also overly strong in both systems relative to the other atomic species (Figure 5 and Table 3).

### 3.3. MN Hya (RX J0929.1+2404)

The interpretation of MN Hya is relatively straightforward. Except for the eclipse, circular polarization varies smoothly from  $-20\%$  to  $+10\%$  through the 3.39 hr period (Buckley et al. 1998b). Our orbit of polarimetry displayed in Figure 7 exhibits this behavior at a time resolution of 45 s ( $\Delta\varphi = 0.004$ ). The presence of both senses of polarization during the orbital cycle indicates a 2-pole accretion system. Ramsay & Wheatley (1998; cf. Buckley et al. 1998b) have proposed a model in which a dominant, positively-polarized pole is hidden behind the stellar limb except during the interval  $0.45 \lesssim \varphi \lesssim 0.75$ . A weaker, negatively-polarized pole is visible between  $0.65 \lesssim \varphi \lesssim 0.25$  and responsible for the strong polarization around the time of eclipse. Though a portion of our optical light curve is complicated by the passage of clouds, the polarization curve is unaffected and consistent with this interpretation. Furthermore, the S-wave in circular polarization in the interval  $\varphi = 0.4 - 0.55$  can be explained in this model as the successive disappearance of the negative pole and appearance of the positive pole over the white dwarf limb, with the double sign change due to viewing each of the slightly elevated shocks “from below” (ref. the polarization undershoot in VV Pup; Liebert & Stockman 1979). A flux minimum at this time is consistent with the grazing viewing aspect of both accretion regions.

Our single epoch of FOS spectroscopy of MN Hya presented in Figure 2 shows sharp, well-defined transitions in the white-light and NUV bands, indicating a compact cyclotron-emitting shock. Very little flux is detected in

the two high-frequency channels. The light curves closely resemble optical eclipse profiles measured by Buckley et al. (1998a) but are quite unlike the X-ray light curve (Buckley et al. 1998b), where a broadened eclipse and hardening of the spectrum indicates absorption by the intervening accretion stream. In Figure 8 the FOS white-light and NUV curves are compared to an eclipse profile obtained on 1996 Mar. 10 with the MMT using a CCD continuously clocked at a rate of 7.8 rows  $s^{-1}$ . In the latter curve, the effective time resolution is set by the FWHM of the seeing profile at  $\Delta t \sim 0.7$  s, similar to the FOS data. Ingress and egress of the bright spot are measured from the optical light curves as  $\Delta t(c_1, c_2) = 2$  s, and  $\Delta t(c_3, c_4) = 3$  s, i.e. essentially unresolved. The implied linear dimension on the white dwarf is  $\lesssim 1 \times 10^8$  cm ( $f_{cyc} \lesssim 0.004$ ).

A non-zero flux and concave profile through minimum light is common to at least the white-light and NUV channels. The UV spectrum from the eclipse interval,  $0.987 < \varphi < 0.024$ , shown in Figure 9, exhibits strong emission lines superposed on a weak, rather red, continuum. Clearly, a small portion of the stream remains exposed even at mid-eclipse. The extinction correction for MN Hya was based on the out-of-eclipse spectrum and amounts to only  $A_V = 0.10 \pm 0.05$  mag. It is important to note that, like V1309 Ori, MN Hya is characterized by an unusually strong N V  $\lambda 1240$  line, with the flux ratio N V  $\lambda 1240$ /C IV  $\lambda 1549 = 3.0$ . Once again, N IV  $\lambda 1718$  appears to be present. When gauged according to the N V/C IV, N V/Si IV ratios, MN Hya falls in the gap between the extreme objects BY Cam and V1309 Ori, and the remaining 9 mCVs available to Bonnet-Bidaud & Mouchet (1987), all of which have N V  $\lambda 1240$ /C IV  $\lambda 1549 < 1$ , N V  $\lambda 1240$ /Si IV  $\lambda 1397 < 3$ . To that latter group we can add UZ For and ST LMi (Paper II), and V2301 Oph and V1432 Aql (Szkody & Silber 1996; Friedrich, Staubert, & la Dous 1996a; this study – Table 3). Thus, the emission-line spectra of BY Cam, V1309 Ori, and to a lesser extent, MN Hya, remain anomalous.

### 3.4. V2301 Oph (1H 1752+081)

With the lowest mean surface field yet measured for any AM Her system ( $B \sim 7$  MG), V2301 Oph is probably synchronized only because it is also very compact ( $P = 1.88$  hr). The suggestion that the binary may house a small accretion disk (Silber et al. 1994) has not found support in subsequent studies, all of which indicate a system accreting solely via a stream (Barwig, Ritter, & Bärnbantner 1994; Ferrario et al. 1995; Hessman et al. 1997; Simić et al. 1998; Steiman-Cameron & Imamura 1999). With such a weak field, circular polarization has eluded detection, and thus far there is no indication of the orientation of the white dwarf within the binary.

The UV light curves shown in Figure 3 record one clean ingress but only the latter portion of egress<sup>4</sup>. In the expanded plot shown as Figure 10, ingress in the optical and NUV is seen to be composed of a well-resolved ledge beginning at  $\varphi = 0.972$  and a final decline to minimum light at  $\varphi = 0.993$ . From nearly coincident optical and X-ray photometry, Steiman-Cameron & Imamura (1999) showed that the X-ray eclipse is complete, with ingress occurring during the optical ledge and X-ray egress near  $\varphi = 0.03$ .

The totality of eclipse at short wavelengths is confirmed by our NUV, FUV, and C IV light curves. In addition, the dereddened ( $A_V = 0.25 \pm 0.05$  mag) eclipse spectrum shown in Figure 11 exhibits neither significant continuum nor line emission. The optical decline that extends from  $\varphi \sim 0.972$  to 0.993 implies a source much larger than the white dwarf, and was interpreted by Steiman-Cameron & Imamura (1999) to be the extinguishing of the prograde portion of the accretion stream. The idea is verified by the similarity to our C IV light curve over this phase interval. We return to this point below.

In Figure 10 we identify contact points  $c_1$  and  $c_2$  with ingress and egress of the ledge in the NUV, and measure a time interval  $19 \pm 4$  s or  $\Delta\varphi = 0.0028 \pm 0.0006$ . This is significantly shorter than the  $\sim 50$  s duration measured in a broad optical bandpass by Steiman-Cameron & Imamura (1999), but is still comparable in size to the disk of a white dwarf ( $\sim 9 \times 10^8$  cm), and we follow their assignment as such. Within this interval, points  $c_1'$  and  $c_2'$  mark the contacts of a precipitous drop in the FUV flux which is strong evidence for an accretion-heated spot on the stellar surface. The ingress interval of  $3.0 \pm 1.5$  s implies a linear distance of  $\sim 1.4 \times 10^8$  cm, or a covering factor for a circular spot of  $f_{spot} \sim 0.008$ . The amplitude of the drop,  $\sim 4.4$  counts sample $^{-1}$ , corresponds to a decline in (dereddened) flux of  $\Delta F_\lambda = 7.7 \times 10^{-15}$  ergs  $cm^{-2} s^{-1} \text{Å}^{-1}$ . For  $D = 150 \pm 27$  pc (Silber et al. 1994), the spot brightness temperature is  $T_{spot} \sim 90,000$  K.

Out of eclipse, the *HST* light curves covering  $0.9 < \varphi < 0.15$  show a nearly constant flux level in the NUV and white-light bands, a slow decline in the FUV, and steady rise in line emission. These features can be explained by a geometry in which the dominant pole is receding toward the stellar limb during the eclipse interval, causing a reduction in FUV flux due to foreshortening, but a rise in the line emission as the roughly radial, optically-thick funnel presents an increasing cross-section to our view. The implication is that the orientation of the magnetic axis of the white dwarf within the binary is more closely orthogonal to than it is aligned with the stellar line of centers.

The protracted ingress of the accretion stream, which extends nearly to phase zero or some 140 s beyond eclipse of the white dwarf, is a valuable diagnostic of the extent that the accretion stream overshoots in azimuth the white dwarf. Such a path is of course expected for gas traveling in a purely ballistic trajectory (Lubow & Shu 1975). The simultaneous and rather abrupt fall to zero light in all bands indicates that the final ingress truly defines an “edge” to the gas, as opposed to a gradual thinning out (cf. the eclipse profiles of V1309 Ori in Figures 1 and 6). The implied extension of the emitting gas above the white dwarf is  $7 \times 10^9$  cm, or  $\sim 9 R_{wd}$ . Lubow & Shu characterize stream paths for gas unaffected by magnetic fields according to the point of closest approach from the accreting star,  $\omega_{min}$ , and the radius of the disk that would ensue,  $\omega_d$ . For a non-disk system, we would expect that the maximum projected altitude of the stream above the white dwarf at the time of eclipse would lie intermediate between these characteristic heights. Using parameters estimated for V2301 Oph ( $M_1 = 0.9 M_\odot$ ,  $M_2 = 0.185 M_\odot$ ; Barwig et al. 1994), we find  $\omega_{min} \approx 6 \times 10^9$  cm and

<sup>4</sup>Note that the ephemeris of Barwig et al. (1994) places  $\varphi = 0.0$  prior to the center of minimum light, as has been found in other studies.

$\omega_d \approx 9 \times 10^9$  cm, which indeed bracket the measured extent above. It should be noted that because of the dynamical nature of the stream/magnetosphere interaction, this height might change with time, e.g. with varying accretion rate (cf. the variable,  $4 - 5 R_{\text{wd}}$  height measured by Steiman-Cameron & Imamura 1999). Variations in the shape of stream egress in the interval  $0.03 < \varphi < 0.05$  can be appreciated by an intercomparison of the curves of Steiman-Cameron & Imamura (1999) and to the white-curve in Figure 3.

### 3.5. V1432 Aql (RX J1940.1–1025)

#### 3.5.1. Background

Asynchronous AM Her systems have proven to be interesting puzzles. The prototype, V1500 Cyg (Stockman, Schmidt, & Lamb 1988), was unusually straightforward because it had already accumulated a rich photometric record due to its 1975 nova outburst (e.g., Patterson 1979) and the system accretes continuously onto both magnetic poles. Among the subsequent 3 discoveries<sup>5</sup>, it has been more common to find periods that are sidebands and/or harmonics of the underlying  $P_{\text{spin}}$  and  $P_{\text{orb}}$  due to pole-switching and migration of the accretion footpoints through the lap period (see Ferrario & Wickramasinghe 1999 and Mouchet, Bonnet-Bidaud, & de Martino 1999 for recent discussions). The bright and highly-polarized BY Cam, for example, required study over a period of several years, including an intense photometric campaign, to clearly isolate the spin period of the white dwarf (Silber et al. 1992, 1997). The presence of an eclipsing system among the known asynchronous mCVs is a particular bonus because successive light curves portray an advancing configuration between the stream and stellar magnetosphere. An extensive observational program could in principle track not only the accretion footpoint(s) across the white dwarf but also the gas trajectory which gives rise to those variations. Such information would be invaluable in forming a general understanding of the processes which couple the accreting gas to the magnetic field. V1432 Aql thus occupies a position of unique importance for all mCVs.

Because it is eclipsing, the binary period of V1432 Aql is unequivocal at 3.365 hr. However, controversy immediately arises over the origin of the eclipses, and they have been more commonly labeled “dips” to reflect this uncertainty. Watson et al. (1995) noted phase jitter as well as an offset between the optical/X-ray dips and the velocity zero-crossing of the emission lines in proposing that the dips are due to obscuration by a high-density accretion stream. An extensive photometric campaign by Patterson et al. (1995) led to the identification of a superposed periodicity at 3.375 hr, taken to be the spin period of the white dwarf and implying a lap period of 50 d. However, the secondary star was preferred as the eclipsing object. Several ensuing studies (e.g., Friedrich et al. 1996b; Staubert et al. 1995; Geckeler & Staubert 1997) have supported and extended the duality of periods, but have returned to an eclipse by the stream (but see Geckeler & Staubert 1999). Recently, even the period identification was called into question after another variation at  $\sim \frac{1}{3}$  the orbital period was noted in archival X-ray data (Mukai

1998). The defining measurement – detection of phase-modulated circular polarization – consists only of unpublished data (from Buckley, quoted by Watson 1995) which appears to support the period assignment of Patterson et al. (1995).

#### 3.5.2. New Results

Four epochs of FOS spectroscopy were attempted of V1432 Aql; unfortunately the final observation was lost due to an on-board tape recorder failure. Overall, the data span  $\sim \frac{1}{3}$  of a 50 d lap cycle. As shown in Figure 4, dip ingress and egress were each recorded on only one occasion. The light curves vary enormously among themselves and are quite unlike those of the other eclipsing systems. At all epochs a downward inflection is apparent near  $\varphi = 0.96$ , at approximately the phase of optical ingress (e.g., Watson et al. 1995). However, the duration of this transition varies with epoch and FOS waveband from  $\Delta\varphi \sim 0.03$  (360 s) for all continuum bands on 19 Aug. 1996 to  $\Delta\varphi \sim 0.005$  (60 s) for the FUV approximately 2 weeks later. The dips approach totality only in the FUV, and even here significant signal remains at minimum light for all but the 3 Sep. observation. The phase of optical egress,  $\varphi = 0.035$ , is barely covered on 29 Aug., but there is no indication of a sharp inflection in any of the spacecraft bands at this time; indeed the data are consistent with a smooth rise in count rate from the brief minimum around  $\varphi = 0.98$ . By contrast, the emission-line channel shows no evidence of dips at all, with only a gradual, ill-defined fading through the observation of 19 Aug. The data from this epoch were also searched for spectral shifts in the centroid and shape of C IV  $\lambda 1549$  during the “ingress” period  $0.96 \lesssim \varphi \lesssim 0.00$ , such as might occur from the eclipse of a disk. No such variations were detected to a limit of about one diode ( $\sim 600 \text{ km s}^{-1}$ ).

The top panel of Figure 12 presents the pipeline-processed spectrum of V1432 Aql averaged over all epochs. The plot basically resembles the single *IUE* spectrum obtained by Friedrich et al. (1996a). However, two new features are evident in the much higher quality FOS data: a prominent 2200 Å depression, and the presence of Ly $\alpha$  in absorption. The interstellar absorption feature can be erased cleanly for a visual extinction  $A_V = 0.7 \pm 0.1$  mag. Eclipse ( $\varphi = 0.974 - 0.006$ ) and post-eclipse ( $0.027 - 0.103$ ) spectra corrected for this effect are shown in the bottom panel of Figure 12, both taken from the run on 29 Aug. 1996, and line strengths computed from the mean dereddened spectrum are listed in Table 3. A total extinction of  $A_V = 0.7$  mag is by far the largest found among the objects studied here, but in good agreement with a value of 0.6 mag derived from the Burstein & Heiles (1982) maps for  $l = 29^\circ 0$ ,  $b = -15^\circ 5$ . The implied neutral hydrogen column is  $N_H \sim 1.3 \times 10^{21} \text{ cm}^{-2}$ , and the corresponding equivalent width (EW) of damped Ly $\alpha$  is  $\sim 25 \text{ \AA}$  (Wolfe et al. 1986). Thus, the interstellar medium is an important contributor to the deep absorption feature we detect. We have added a sequence of panels to the light curves in Figure 4 depicting the EW of the Ly $\alpha$  line. In these plots,  $\text{EW} > 0$  corresponds to an absorption line,  $\text{EW} < 0$  indicates emission, and the measurements have been smoothed with a running-mean of width 40 s ( $\Delta\varphi = 0.003$ ). This

<sup>5</sup>BY Cam; V1432 Aql; CD Ind=RX J2115–5840=EUVE J2115–586

index measures the net strength of the feature, since these low resolution data do not resolve the absorption component from any emission line due to the gas stream. Note that the feature shows roughly constant EW except for phase intervals when the FUV flux is near zero – i.e.  $0.965 \lesssim \varphi \lesssim 0.000$  during the deep dips of 29 Aug. and 3 Sep.

### 3.5.3. The UV Continuum Source

The dereddened out-of-eclipse spectrum in Figure 12 exhibits a continuum that rises smoothly to the blue, somewhat flatter than Rayleigh-Jeans. When compared to blackbodies, a temperature of  $T \sim 35,000$  K is found to reproduce the UV slope and not exceed the dereddened optical continuum of the only published spectrum of V1432 Aql that is provided in absolute units (Patterson et al. 1995). To compute the size of the object with this effective temperature, the distance estimate of  $\sim 230$  pc (Watson et al. 1995) must be reduced by 16% to  $\sim 200$  pc to account for the implied 0.3 mag of *I*-band extinction, where detection of the M4 V secondary was made. For a circular object, the UV-optical source is then estimated to have a radius  $R \sim 1.3 \times 10^9$  cm. If white dwarf model atmospheres are used instead (Bergeron 1994), a somewhat lower temperature,  $T = 25,000 - 30,000$  K, and larger size,  $R \sim 1.6 \times 10^9$  cm, ensue. The model atmospheres also predict a Ly $\alpha$  absorption feature with an EW of 30 Å or more which would blend with the interstellar component at this resolution.

The similarity of the derived source size to the disk of a white dwarf is very attractive, and at face value suggests a low-mass star ( $M_{\text{wd}} = 0.15 - 0.25 M_{\odot}$ ). However, there is significant latitude in the combined uncertainties of the extinction correction and distance estimate. Moreover, the white dwarf need not supply the entire observed continuum in either the UV or optical (note the residual flux level in the eclipse spectrum of Figure 12). Thus, a smaller stellar size (larger mass) is possible. A somewhat smaller size,  $R \sim 6 \times 10^8$  cm, is also indicated by the 40 s duration of the most abrupt FUV eclipse ingress on 3 Sep. 1996 (Figure 4). The corresponding luminosity for emission by an entire white dwarf with  $T_{\text{wd}} = 30,000 - 35,000$  K is  $L_{\text{wd}} \sim 0.2 - 0.5 L_{\odot}$ , of which  $\sim 2\%$  is intercepted by the secondary star. This illumination amounts to at most 50% of the  $0.02 L_{\odot}$  nuclear luminosity of an M4 dwarf (cf. V1500 Cyg – Schmidt & Stockman 1995), so the brightness modulation at the orbital period due to reprocessing would be expected to be modest<sup>6</sup>. Indeed, the average light curve of Patterson et al. (1995) shows a  $\sim 0.5$  mag variation away from the dip feature, peaking near  $\varphi = 0.5$ , as is appropriate for an origin on the inner hemisphere of the companion (see the discussion of this point by Patterson et al.). A contribution from the white dwarf and illuminated secondary is also consistent with the weak level of optical circular polarization measured for V1432 Aql ( $|v| \sim 2\%$ , Friedrich et al. 1996b; Watson 1995). Because a hot white dwarf can account for the basic characteristics of the UV-optical spectral energy distribution and is consistent with the mean optical light curve and polarization, we adopt this explanation throughout the remainder of the paper.

### 3.5.4. Origin of the Dips

With the observed energy distribution from the UV through the optical dominated by the hot white dwarf, we now investigate the origin of the photometric dips. Discussion on this topic has centered around the regularity of the features, their depth in various wavelength regions, the duration of ingress/egress, and their phasing relative to other indicators of orbital motion. Secondary star proponents point out the very predictable dip ephemeris and phasing relative to the emission-line radial velocities (Patterson et al. 1995). Gas stream advocates, on the other hand, note an energy dependence of eclipse depth in X-rays and the ingress/egress intervals, which exceed those expected for the sharp-edged eclipse of a white dwarf (Watson et al. 1995; Friedrich et al. 1996b; Geckeler & Staubert 1997).

New information on this question is provided by the FOS spectroscopy. First, the dips in Figure 4 are seen to be highly variable in both *shape* and *depth* from epoch to epoch. Note in particular the absence of a defined ingress on 19 Aug., the lack of an expected egress on 30 Aug., and the variable depth at minimum light. Such behavior is natural for absorption due to a dense, ill-defined gas stream but at odds with a stellar eclipse. This is particularly true for the FUV channel, which from our prior conclusions is dominated by the hot white dwarf. Indeed, based on our results for UZ For (Paper II) and the other systems studied here, it is difficult to imagine any source of appreciable light in the  $\sim 1250 - 1520$  Å region that would not be located on or very near the white dwarf. Second, the UV emission lines are essentially *undiminished* through the absorption dips. This fact has already been noted for the optical lines by Watson et al. (1995) and contested by Patterson et al. (1995; see their Figures 12 and 13). The issue revolves around the various line components and their places of origin. In the case of the high-ionization lines of C IV and He II, the lack of eclipse features in Figure 4 is unequivocal. We also point out that if the white dwarf were being eclipsed by a secondary which fills its Roche lobe, the observed duration of the dip (820 s or  $\Delta\varphi = \pm 0.035$ ) requires an inclination  $i \geq 78^\circ$ . In this case, the eclipse track crosses behind the secondary disk  $\sim \frac{2}{3}$  of the way from the center. The remainder of the disk would be expected to obscure line-emitting gas in the lower accretion streams(s) out to  $\sim 7 R_{\text{wd}}$  above the orbital plane for a period of up to  $\sim 800$  s. No such reduction in emission-line light is evident.

We therefore conclude that the absorption dips in V1432 Aql are due to the intervention of a dense portion of the accretion flow. In the context of emission by a white dwarf disk and eclipse by a stream, the curious “choppy” appearance to the light curves *at all orbital phases* (Watson et al. 1995; Patterson et al. 1995) is suggestive of persistent obscuration by gas clumps, such as might occur in a circulating accretion “ring”. A similar structure is inferred to exist in the asynchronous mCV V1500 Cyg from its ever-present sinusoidal polarization curve that implies 2-pole accretion (Schmidt, Liebert, & Stockman 1995). We also note that the lack of an identifiable eclipse by the secondary implies that the inclination of V1432 Aql is  $i < 73^\circ$ . A very rough estimate can also be gained from the

<sup>6</sup>And dependent on the unknown system inclination.

observed radial velocity half-amplitude of the narrow emission lines ( $160 \text{ km s}^{-1}$ ; Patterson et al. 1995), which for reasonable white dwarf and secondary star masses ( $\sim 0.6$  and  $0.3 M_{\odot}$ , respectively) suggests  $i \sim 40^{\circ}$ .

#### 4. V1432 Aql AS A RECENT NOVA

The link between the nova event and asynchronism was established with the discovery that the 1975 nova system V1500 Cyg is an mCV (Stockman et al. 1988). In support of this position, Patterson et al. (1995) has pointed out the vanishing likelihood that all 4 asynchronous systems would be synchronizing for the first time, given that the spin-orbit period difference is universally  $\sim 1\%$  and that, when measured, locking timescales are all in the range  $10^2 - 10^3 \text{ yr}$  (Schmidt et al. 1995; Mason et al. 1995; Geckeler & Staubert 1997). The likely alternative is that most, if not all, of the asynchronous AM Her systems were previously phase-locked and that the magnetic connections were broken in recent nova events.

Only in the case of V1500 Cyg is the post-nova classification certain. The object has an extremely rich observational history post-1975, the white dwarf temperature has been measured at  $T_{\text{wd}} \sim 90,000 \text{ K}$  and decreasing, and the object lies at the center of an expanding debris shell. None of the other asynchronous systems have been associated with a nebula, despite searches. The likelihood that the aforementioned abundance anomalies of BY Cam (§3.2.) are indicative of mixing with nova-processed material is reduced now that the synchronized systems V1309 Ori and MN Hya have been found to show elevated N V line strengths. A nova event in the recent past of the 8 hr-period V1309 Ori appears particularly improbable, as it should be especially easy to disrupt and slow to resynchronize.

Excluding V1500 Cyg, the temperature of  $\sim 35,000 \text{ K}$  that we have measured for the white dwarf in V1432 Aql is far and away the hottest yet found on an AM Her system (Sion 1999; Gänsicke 1999). When all CVs are considered, white dwarfs this hot have been detected *only* in dwarf nova and nova-like classes (Sion 1999), both of which are thought to be eruptive. It is therefore tempting to classify V1432 Aql as the second post-nova AM Her system. Using the cooling calculations of Prialnik (1986) as a guide, the current stellar luminosity of  $0.2 - 0.5 L_{\odot}$  for V1432 Aql vs.  $\sim 5 L_{\odot}$  for V1500 Cyg (Schmidt et al. 1995) suggests that the interval since the last eruption of V1432 Aql is in the range  $\Delta t = 75 - 150 \text{ yr}$ . At a distance  $D \sim 200 \text{ pc}$  and an expansion velocity  $v = 1000 \text{ km s}^{-1}$ , the shell could now be several arcminutes across. Because the surface brightness of a nebular remnant scales as  $(v\Delta t)^{-5}$  (Cohen 1988)<sup>7</sup>, direct imaging of it might be very difficult (see also Wade 1990). We note that the faintness and lack of a hot blackbody component in the near-UV spectrum of BY Cam (Bonnet-Bidaud & Mouchet 1987; Shrader et al. 1988) suggest that, if it is also a post-nova system, it is considerably older still and thus detection of a shell would be hopeless.

The fly in the ointment for a post-nova explanation of V1432 Aql is the fact that in this case  $P_{\text{spin}} > P_{\text{orb}}$ . The mechanism outlined by Stockman et al. (1988) for decoupling V1500 Cyg involved the transfer of a small amount

of orbital angular momentum to the bloated white dwarf during the common-envelope phase of the nova. When the photosphere contracted back within the binary and eventually to a normal stellar radius, the two motions could be distinguished observationally, and  $P_{\text{spin}} < P_{\text{orb}}$ . To achieve the V1432 Aql configuration from an outburst in an initially synchronized binary requires either decreasing the orbital period of the binary (such that the secondary spirals inward) or increasing the spin period of the primary. Shara et al. (1986) has shown that the net effects of frictional angular momentum loss on a secondary orbiting within the envelope results in a decrease in the binary dimension  $a$  only for slow novae with very low-mass secondaries ( $M_2/M_{\text{wd}} \lesssim 0.01$ ). Of course, for V1432 Aql, it is not sufficient merely that  $\Delta a < 0$ , but that the resulting decrease in  $P_{\text{orb}}$  exceed the decrease in  $P_{\text{spin}}$  due to spin-up of the envelope (the V1500 Cyg effect). Thus, an explanation of the sense of asynchronism of V1432 Aql purely in terms of dynamical effects is not likely.

More promising is rotational braking of the white dwarf during the mass-loss phase via the strong magnetic field (the magnetic propeller effect). This problem has been presented in many ways for single stars as well as members of binary systems. We choose the convenient formulation of Kawaler (1988), which can be expressed in terms of the fractional change in rotational angular momentum

$$\frac{\Delta J}{J} = \frac{5}{3} \frac{\Delta M}{M_{\text{wd}}} \left( \frac{r_A}{R_{\text{wd}}} \right)_{\text{radial}}^n \quad (1)$$

Here,  $\Delta M$  is the total mass lost in the eruption,  $r_A$  (radial) is the Alfvén radius out to which corotation is maintained for a radial magnetic field line distribution,  $n$  is an index that denotes the departure from a radial field geometry, and we have approximated the moment of inertia of the white dwarf by that of a uniform-density sphere. A value  $n = 2$  denotes radial field lines, while  $n = 3/7$  is appropriate for a dipole. The expression for  $r_A$  provided by Kawaler (1988) can be rewritten using parameters appropriate for a  $0.6 M_{\odot}$  white dwarf as

$$\left( \frac{r_A}{R_{\text{wd}}} \right)_{\text{radial}} \approx 1.2 \times 10^6 B_0^{4/3} \dot{M}^{-2/3} \quad (2)$$

with  $B_0$  being the surface magnetic field in gauss and  $\dot{M}$  in  $\text{gm s}^{-1}$ . Assuming  $B_0 = 3 \times 10^7 \text{ G}$  and continuous mass loss totalling  $\Delta M = 10^{-4} M_{\odot}$  over a wind phase of  $\Delta t = 10^7 \text{ s}$  (MacDonald, Fujimoto, & Truran 1985), we find a decoupling radius for radial field lines  $r_A$  (radial)  $\sim 15 R_{\text{wd}}$ , well inside the orbit of the secondary. The total angular momentum lost is then  $\Delta J/J = 0.001 - 0.06$ , with the two limits signifying dipolar and radial geometries, respectively. The consistency with the 0.3% period difference currently observed for V1432 Aql is encouraging.

The above derivation is admittedly crude. It serves, however, to illustrate the possible importance of magnetic braking during the outburst. In view of this result, it might be better to view V1500 Cyg as an example, rather than a template, of a nova eruption in an mCV, and given that the net outcome is the result of a competition between at least two effects with magnitudes of a few percent each, a system  $P_{\text{spin}} > P_{\text{orb}}$  might also be expected. In fact, with  $r_A$  being most sensitive to the magnetic field strength and duration of the wind phase ( $\propto B_0^{4/3} \Delta t^{2/3}$ ),

<sup>7</sup>The dependence is even steeper if the nebula is ionization-bounded.



a very fast nova like V1500 Cyg could experience spin-up, while a higher-field, slow nova might be spun down.

## 5. CONCLUSIONS

Time-resolved *HST* UV spectroscopy of four eclipsing mCVs has enabled us to identify:

- Accretion-heated photospheric spots in V1309 Ori and V2301 Oph with covering factors  $f < 0.015$  and  $\sim 0.008$ , and blackbody temperatures  $T_{\text{spot}} > 150,000$  K and  $\sim 90,000$  K, respectively.
- A cyclotron shock on MN Hya with  $f \lesssim 0.004$ .
- Prominent emission from the accretion stream in V1309 Ori and V2301 Oph. A protracted emission-line ingress in the latter object indicates the stream penetrates the magnetosphere to a height of  $\sim 9 R_{\text{wd}}$  before it is funneled onto the magnetic poles.
- Unusually strong N V  $\lambda 1240$  in V1309 Ori and, to a lesser extent, MN Hya, that is suggestive of an overabundance of nitrogen in the gas stream.
- A spectral energy distribution for V1432 Aql that strongly suggests the dominant source of energy is a hot ( $T_{\text{wd}} \sim 35,000$  K) white dwarf. The undiminished line emission through eclipse indicates that the eclipse is caused by a dense portion of the accretion stream, not the secondary star. The very hot white dwarf, combined with the current asynchronous nature and rapid timescale for relocking, suggests that V1432 Aql underwent a nova eruption in the past  $\sim 75 - 150$  yr. A reversed sense of asynchronism, with the primary star currently spinning up toward synchronism, is not at odds with this history, if the white dwarf rotation can magnetically couple to the ejecta during the dense wind phase of the eruption.

Time-tagged UV spectrophotometry is an important tool for understanding the sizes and relative contributions of the accretion stream, hot spot, and white dwarf photospheres in mCVs. Both the Space Telescope Imaging Spectrograph (STIS) and the Cosmic Origins Spectrograph (COS) offer sensitivities an order of magnitude greater than the FOS. Unfortunately, with the limited aperture of *HST*, it will be difficult to resolve objects smaller than 10% of the white dwarf radius. Future UV telescopes, with apertures exceeding 4 m and high efficiency, energy-resolving detectors will be ideal facilities for discerning details of structures as small as the accretion shock itself.

Special thanks go to Carolyn Pointek for assistance with the initial data analysis and to R. Wagner for spearheading the development of high-speed CCD photometry at the MMT and for lending assistance at the telescope. P. Bergeron kindly provided DA model atmosphere spectra. Support was provided through NASA grant GO-6498 from the Space Telescope Science Institute, which is operated by the Association of Universities for Research in Astronomy, Inc., under NASA contract NAS 5-26555. Ground-based studies of magnetic stars and stellar systems are funded by NSF grant AST 97-30792 to GDS.

## REFERENCES

- Barwig, H., Ritter, H., & Bärnbantner, O. 1994, *A&A*, 288, 204
- Bergeron, P. 1994, private communication
- Beuermann, K., & Woelk U. 1996, in *Proc. IAU Colloq. 158, Cataclysmic Variables and Related Objects*, ed. A. Evans & J.H. Wood (Dordrecht: Kluwer), 199
- Bonnet-Bidaud, J.M., & Mouchet, M. 1987, *A&A*, 188, 89
- Buckley, D.A.H., Barrett, P.E., Haberl, F., & Sekiguchi, K. 1998a, *MNRAS*, 299, 998
- Buckley, D.A.H., Ferrario, L., Wickramasinghe, D.T., & Bailey, J.A. 1998b, *MNRAS*, 295, 899
- Buckley, D.A.H., & Shafter, A.W. 1995, *MNRAS*, 275, L61
- Burstein, D., & Heiles, C. 1982, *AJ*, 87, 1165
- Cardelli, J.A., Clayton, G.C., & Mathis, J.S. 1989, *ApJ*, 345, 245
- Cohen, J. 1988, in *A.S.P. Conf. Series 4, The Extragalactic Distance Scale*, ed. S. van den Bergh & C.J. Pritchett (San Francisco: A.S.P.), 114
- Cropper, M. 1990, *Space Sci. Rev.*, 54, 195
- de Martino, D., Barcaroli, R., Matt, G., Mouchet, M., Belloni, T., Beuermann, K., Chiappetti, L., Done, C., Gaensicke, B.T., La Franca, F., & Mukai, K. 1998, *A&A*, 332, 904
- Ferrario, L., & Wickramasinghe, D.T. 1999, *MNRAS*, 309, 517
- Ferrario, L., Wickramasinghe, D., Bailey, J., & Buckley, D. 1995, *MNRAS*, 273, 17
- Frank, J., Lasota, J.-P., & Chanmugam, G. 1995, *ApJ*, 453, 446
- Friedrich, S., Staubert, R., & la Dous, C. 1996a, *A&A*, 315, 411
- Friedrich, S., Staubert, R., Lamer, G., König, M., Geckeler, R., Bässgen, M., Kollatschny, W., Östreicher, R., James, S.D., & Sood, R.K. 1996b, *A&A*, 306, 860
- Gänsicke, B.T. 1999, in *ASP Conf. Proc. 157, Annapolis Workshop on Magnetic Cataclysmic Variables*, ed. C. Hellier & K. Mukai (San Francisco: ASP), 261
- Garnavich, P.M., Szkody, P., Robb, R.M., Zurek, D.R., & Hoard, D.W. 1994, *ApJ*, 435, L141
- Geckeler, R.D., & Staubert, R. 1997, *A&A*, 325, 1070
- Geckeler, R.D., & Staubert, R. 1999, Abstracts of Contributed Talks and Posters presented at the Annual Scientific Meeting of the Astronomische Gesellschaft, Vol 15
- Hakala, P.J. 1995, *A&A*, 296, 164
- Harrop-Allin, M.K., Cropper, M., Hakala, P.J., Hellier, C., & Ramseyer, T. 1999a, *MNRAS*, 308, 807
- Harrop-Allin, M.K., Cropper, M., Potter, S.B., Dhillon, V.S., & Howell, S.B. 1997, *MNRAS*, 288, 1033
- Harrop-Allin, M.K., Hakala, P.J., & Cropper, M. 1999b, *MNRAS*, 302, 362
- Hessman, F.V., Beuermann, K., Burwitz, V., de Martino, D., & Thomas, H.-C. 1997, *A&A*, 327, 245
- Kawaler, S.D. 1988, *ApJ*, 333, 326
- Kube, J., Gänsicke, B.T., & Beuermann, K. 2000, *A&A*, 356, 490
- Liebert, J., & Stockman, H.S. 1979, *ApJ*, 229, 652
- Lubow, S.H., & Shu, F.H. 1975, *ApJ*, 198, 383
- MacDonald, J., Fujimoto, M.Y., & Truran, J.W. 1985, *ApJ*, 294, 263
- Mason, P.A., Andronov, I.L., Kolesnikov, S.V., Pavlenko, E.P., & Shakovskoy, N.M. 1995, in *ASP Conf. Proc. 85, Cape Workshop on Magnetic Cataclysmic Variables*, ed. D.A.H. Buckley & B. Warner, (San Francisco: ASP), 496
- Mouchet, M., Bonnet-Bidaud, J.-M., & de Martino, D. 1999, in *ASP Conf. Proc. 157, Annapolis Workshop on Magnetic Cataclysmic Variables*, ed. C. Hellier & K. Mukai (San Francisco: ASP), 215
- Mukai, K. 1998, *ApJ*, 498, 394
- Patterson, J. 1979, *ApJ*, 231, 789
- Patterson, J., Skillman, D.R., Thorstensen, J., & Hellier, C. 1995, *PASP*, 107, 307
- Prialnik, D. 1986, *ApJ*, 310, 222
- Ramsay, G., & Wheatley, P.J. 1998, *MNRAS*, 301, 95
- Schmidt, G.D., Liebert, J., & Stockman, H.S. 1995, *ApJ*, 441, 414
- Schmidt, G.D., & Stockman, H.S. 1991, *ApJ*, 371, 749
- Schmidt, G.D., Stockman, H.S., & Smith, P.S. 1992, *ApJ*, 398, L57
- Schmidt, G.D., Weymann, R.J., & Foltz, C.B. 1989, *PASP*, 101, 713
- Schwope, A.D. 1998, in *ASP Conf. Proc. 137, 13th North American Workshop on Cataclysmic Variables and Related Objects*, ed. S. Howell, E. Kuulkers, & C. Woodward (San Francisco: ASP), 44
- Schwope, A.D., Schwarz, R., Staude, A., Heerlein, C., Horne, K., & Steeghs, D. 1999, in *ASP Conf. Proc. 157, Annapolis Workshop on Magnetic Cataclysmic Variables*, ed. C. Hellier & K. Mukai (San Francisco: ASP), 71
- Shafter, A.W., Reinsch, K., Beuermann, K., Misselt, K.A., Buckley, D.A.H., Burwitz, V., & Schwöpe, A.D. 1995, *ApJ*, 443, 319
- Shara, M.M., Livio, M., Moffat, A.F.J., & Orio, M. 1986, *ApJ*, 311, 163
- Shrader, C.R., McClintock, J.E., Remillard, R., Silber, A., & Lamb, D.Q. 1988, in *A Decade of Astronomy with the IUE Satellite*, 1, 137
- Silber, A., Bradt, H.V., Ishida, M., Ohashi, T., & Remillard, R.A. 1992, *ApJ*, 389, 704
- Silber, A.D., Remillard, R.A., Horne, K., Bradt, & H.V. 1994, *ApJ*, 424, 955
- Silber, A.D., Szkody, P., Hoard, D.W., Hammergren, M., Morgan, J., Fierce, E., Olsen, K., Mason, P.A., Rolleston, R., Ruotsalainen, R., Pavlenko, E.P., Shakhovskoy, N.M., Shugarov, S., Andronov, I.L., Kolesnikov, S.V., Naylor, T., & Schmidt, E. 1997, *MNRAS*, 290, 25
- Simić, D., Barwig, H., Bobinger, A., Mantel, K.-H., & Wolf, S. 1998, *A&A*, 329, 115
- Sion, E.M. 1999, *PASP*, 111, 532
- Sohl, K., & Wynn, G. 1999, in *ASP Conf. Proc. 157, Annapolis Workshop on Magnetic Cataclysmic Variables*, ed. C. Hellier & K. Mukai (San Francisco: ASP), 87
- Staubert, R., Friedrich, S., Lamer, G., König, M., & Geckeler, R. 1995, in *ASP Conf. Proc. 85, Cape Workshop on Magnetic Cataclysmic Variables*, ed. D.A.H. Buckley & B. Warner, (San Francisco: ASP), 264
- Steiman-Cameron, T.Y., & Imamura, J.N. 1999, *ApJ*, 515, 404
- Stockman, H.S., & Schmidt, G.D. 1996, *ApJ*, 468, 883 (Paper II)
- Stockman, H.S., Schmidt, G.D., & Lamb, D.Q. 1988, *ApJ*, 332, 282
- Stockman, H.S., Schmidt, G.D., Liebert, J., & Holberg, J.B. 1994, *ApJ*, 430, 323 (Paper I)
- Szkody, P. 1999, in *ASP Conf. Proc. 157, Annapolis Workshop on Magnetic Cataclysmic Variables*, ed. C. Hellier & K. Mukai (San Francisco: ASP), 195
- Szkody, P., & Silber, A. 1996, *AJ*, 112, 289
- Vrieland, S., & Schwöpe, A.D. 1999, in *ASP Conf. Proc. 157, Annapolis Workshop on Magnetic Cataclysmic Variables*, ed. C. Hellier & K. Mukai (San Francisco: ASP), 93
- Wade, R.A. 1990, in *Proc. IAU Colloquium 122, Physics of Classical Novae*, ed. A. Cassatella & R. Viotti (Berlin: Springer-Verlag), 179
- Walter, F.M., Scott, J.W. & Adams, N.R. 1995, *ApJ*, 440, 834
- Watson, M.G. 1995, in *ASP Conf. Proc. 85, Cape Workshop on Magnetic Cataclysmic Variables*, ed. D.A.H. Buckley & B. Warner, (San Francisco: ASP), 259
- Watson, M.G., Rosen, S.R., O'Donoghue, D., Buckley, D.A.H., Warner, B., Hellier, C., Ramseyer, T., Done, C., & Madejski, G. 1995, *MNRAS*, 273, 681
- Wolfe, A.M., Turnshek, D.A., Smith, M.G., & Cohen, R.D. 1986, *ApJS*, 61, 249

TABLE 1  
SYSTEM PARAMETERS

System	$P_{\text{orb}}$ (hr)	$D$ (pc)	$A_V$ (mag)	$\beta^{\text{a}}$	$\psi^{\text{b}}$	$B$ (MG)	Refs.
V1309 Ori	7.98271	>500(>1500?)	$0.15 \pm 0.05$	...	$\sim 90^\circ$	61	3,5,7,10
MN Hya	3.38985	300 – 700	$0.10 \pm 0.05$	$\sim 30^\circ$	$\sim 0^\circ$	20: 42:	2,9,13
V2301 Oph	1.88280	$150 \pm 27$	$0.25 \pm 0.05$	$15^\circ - 30^\circ$	...	7	1,4,11
V1432 Aql	3.36564	180 – 250	$0.7 \pm 0.1$	$\sim 58^\circ?$	asynchronous	...	6,8,12,13

<sup>a</sup>Colatitude of accretion region

<sup>b</sup>Azimuth of accretion region

References. — (1) Barwig et al. (1994); (2) Buckley et al. (1998b); (3) Buckley & Shafter (1995); (4) Ferrario et al. (1995) (5) Garnavich et al. (1994); (6) Geckeler & Staubert (1997); (7) Harrop-Allin et al. (1997) (8) Patterson et al. (1995); (9) Ramsay & Wheatley (1998); (10) Shafter et al. (1995); (11) Silber et al. (1994); (12) Watson et al. (1995); (13) this paper.

TABLE 2  
OBSERVING LOG

System	UT Date	HJD Start–End (2450000+)	Type <sup>a</sup>	Comment
V1309 Ori (RX J0515.6+0105)	1996 Aug 4	299.9656 – .9725	OS	$V \sim 16.5$ @ $\varphi = 0.33$
	1996 Aug 12	307.80673 – .81753	US	
	1996 Aug 22	318.12780 – .13943	US	
	1996 Aug 22	318.14311 – .15359	US	
	1996 Aug 24	320.13874 – .15037	US	
	1996 Aug 24	320.15405 – .16453	US	
	1996 Aug 26	322.14953 – .16116	US	
	1996 Aug 26	322.16484 – .17532	US	
	1996 Sep 16	343.39618 – .40701	US	
	1996 Sep 27	353.72920 – .73968	US	
	1996 Oct 1	357.73670 – .74834	US	
	1996 Oct 1	357.75202 – .76249	US	
	1996 Oct 25	382.49924 – .51064	US	
	1996 Oct 26	382.51433 – .52480	US	
	1996 Dec 3	420.8318 – .8422	OS	
MN Hya (RX J0929.1–2404)	1996 Jan 27	109.822 – .970	P,Ph	$v = -17\%$ to $+5\%$ 128 ms time samples Extremely faint Extremely faint $V > 20$ $V \sim 16.9$
	1996 Mar 10	152.790 – .799	Ph	
	1996 Oct 14	371.28629 – .29618	US	
	1996 Oct 14	371.29987 – .30455	US	
	1996 Oct 15	372.02 – .03	OS	
	1996 Dec 4	421.98 – .99	OS	
	1996 Dec 24	442.05640 – .06629	US	
	1996 Dec 24	442.06997 – .07466	US	
V2301 Oph (1H 1752+081)	1996 Aug 3	299.08228 – .09217	US	$V \sim 15.8$ @ $\varphi = 0.42$
	1996 Aug 3	299.14747 – .15217	US	
	1996 Aug 4	299.6543 – .6612	OS	
	1996 Aug 30	325.74371 – .75360	US	
	1996 Aug 30	325.75729 – .76197	US	
V1432 Aql (RX J1940.1–1025)	1996 Aug 19	314.68951 – .70027	US	FGS/tape recorder failure FGS/tape recorder failure
	1996 Aug 29	325.34667 – .35830	US	
	1996 Aug 29	325.36198 – .37245	US	
	1996 Sep 3	330.25291 – .26367	US	
	1996 Sep 9	335.86638 – .87801	US	
	1996 Sep 9	335.88169 – .89217	US	

<sup>a</sup>US = UV spectroscopy; OS = optical spectroscopy; P = optical polarimetry, Ph = optical photometry

TABLE 3  
 UV LINE STRENGTHS<sup>a</sup> ( $\times 10^{-13}$  ergs cm<sup>-2</sup> s<sup>-1</sup>)

Line	V1309 Ori	MN Hya	V2301 Oph	V1432 Aql
C III $\lambda 1176$	...	...	8.2	25.8
Ly $\alpha$ <sup>b</sup> $\lambda 1216$	2.6	3.9	8.3	Absorption
N V $\lambda 1240$	17.4	2.3	13.3	41.8
Si III $\lambda 1298$	1.2	0.35	4.1	4.5
C II $\lambda 1335$	0.32	...	3.8	4.3
O V $\lambda 1371$	0.93	0.14:	...	5.1
Si IV $\lambda 1397$	5.4	1.3	13.3	23.8
C IV $\lambda 1549$	2.4	0.76	29.4	83.4
He II $\lambda 1640$	4.5	0.94	7.2	24.6
N IV $\lambda 1718$	1.6	0.09:	...	1.7
Al III $\lambda 1857$	1.2	0.25	3.8	2.9
C III $\lambda 2297$	0.29:	...	0.87	2.4
He II $\lambda 2383$	0.18:	...	...	1.1

<sup>a</sup>Extinction-corrected

<sup>b</sup>May have a geocoronal emission component

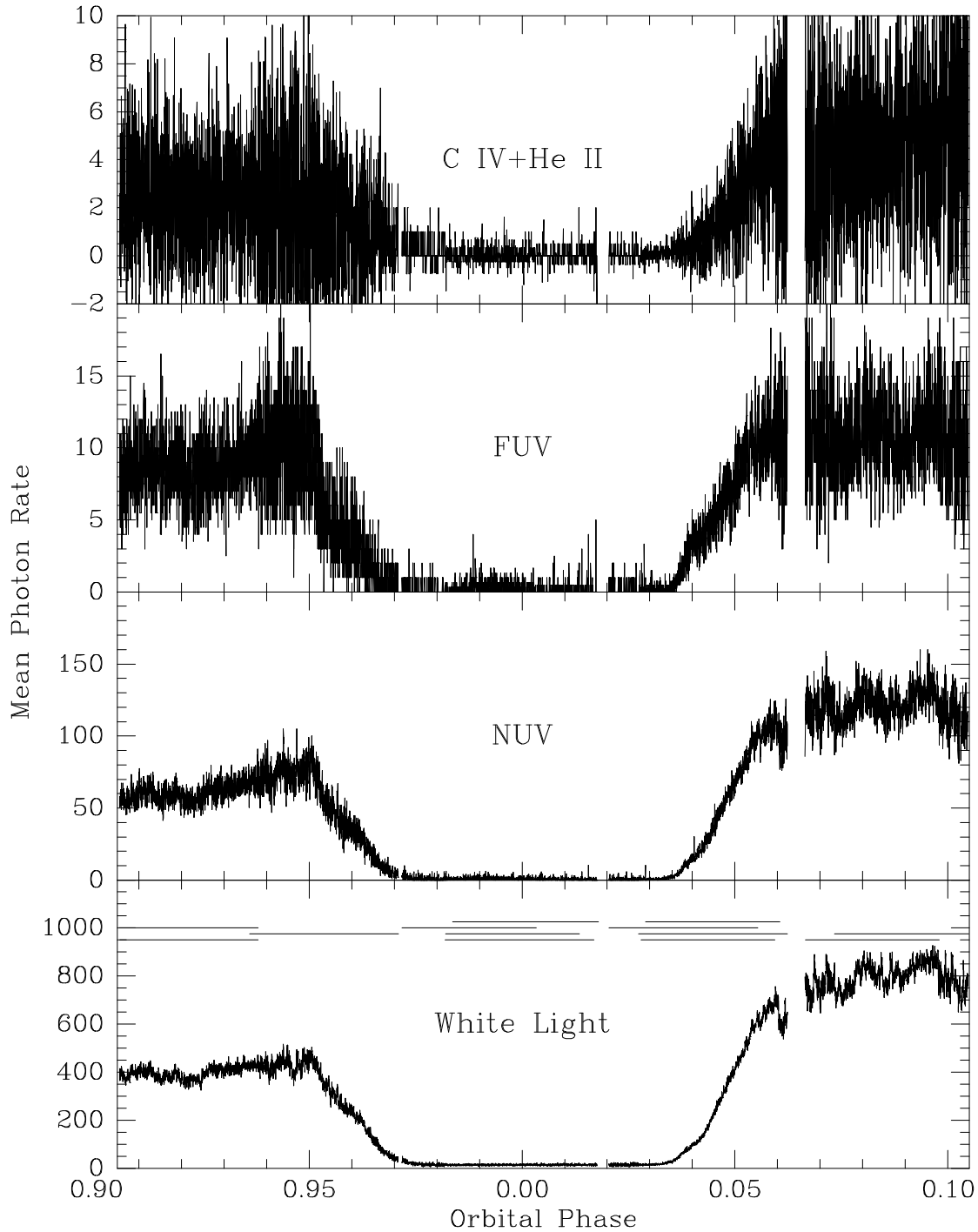


FIG. 1.— *HST* eclipse light curves averaged over all epochs of the magnetic variable V1309 Ori. Panels represent: *C IV+He II*: the C IV  $\lambda\lambda 1548, 1551$  plus He II  $\lambda 1640$  emission lines; *FUV*: the  $\lambda\lambda 1255 - 1518$  continuum; *NUV*: the  $\lambda\lambda 1945 - 2506$  continuum; *White Light*: the zero-order image, a broad passband with  $\lambda_{\text{eff}} \sim 3400\text{\AA}$ . Horizontal line segments in the bottom panel indicate phase intervals of the individual time series. Rate units are detected photon counts per 0.8201 s sample.

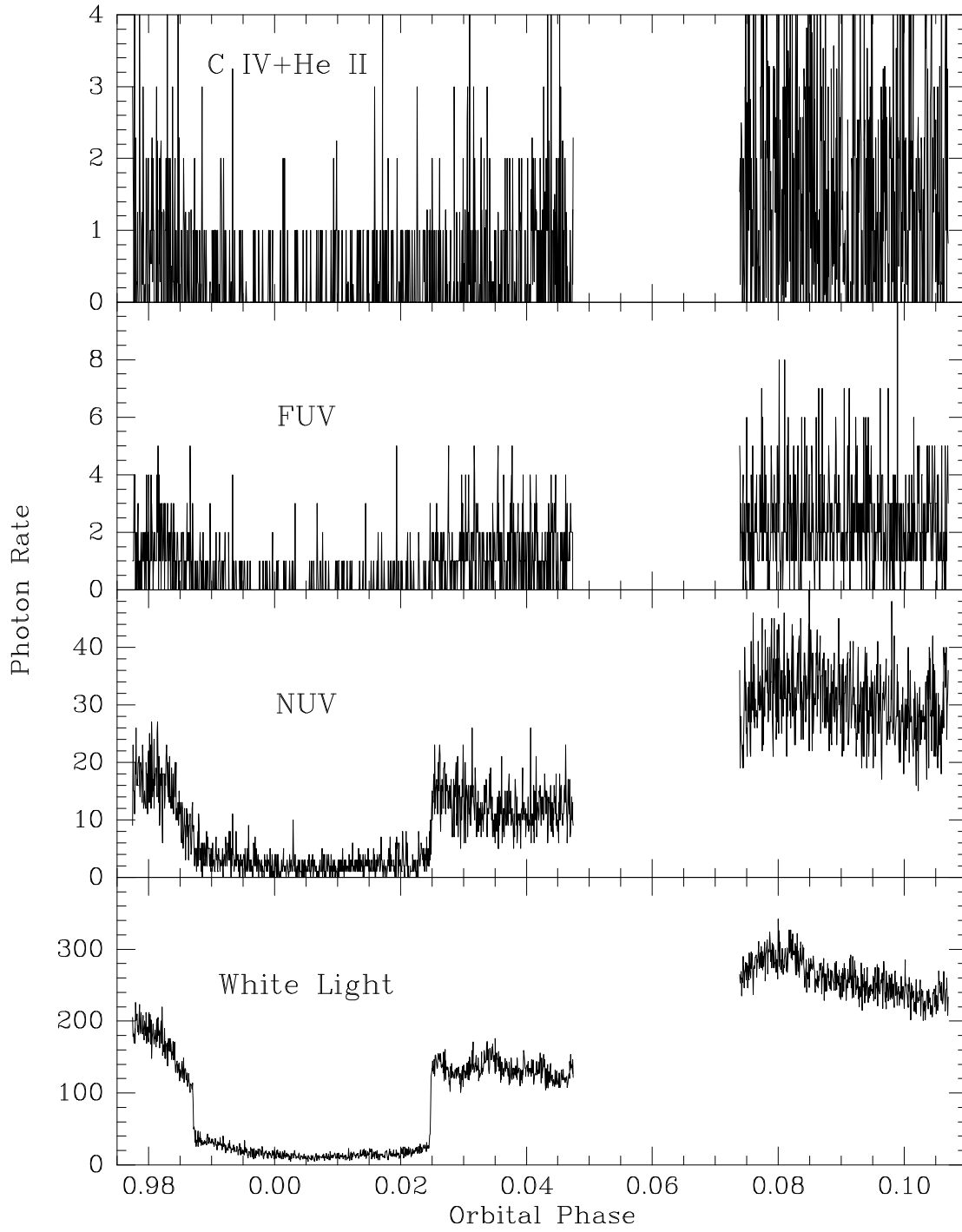


FIG. 2.— As in Figure 1 for MN Hya. Due to the extremely faint state encountered in the initial visit, only data from the second pointing are shown here.

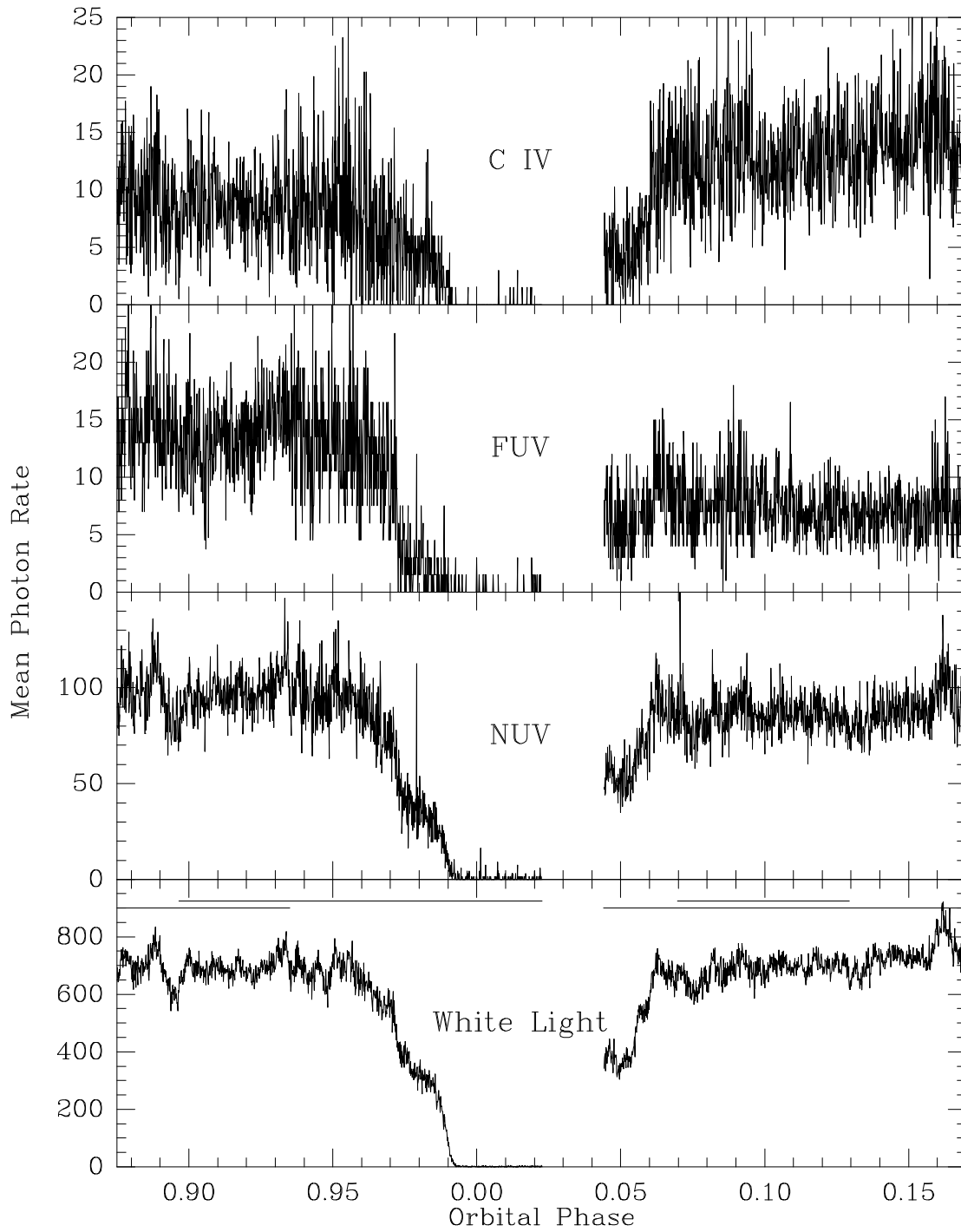


FIG. 3.— As in Figure 1 for V2301 Oph. With C IV  $\lambda 1549$  dominating the UV emission-line spectrum, its flux alone is displayed in the top panel.



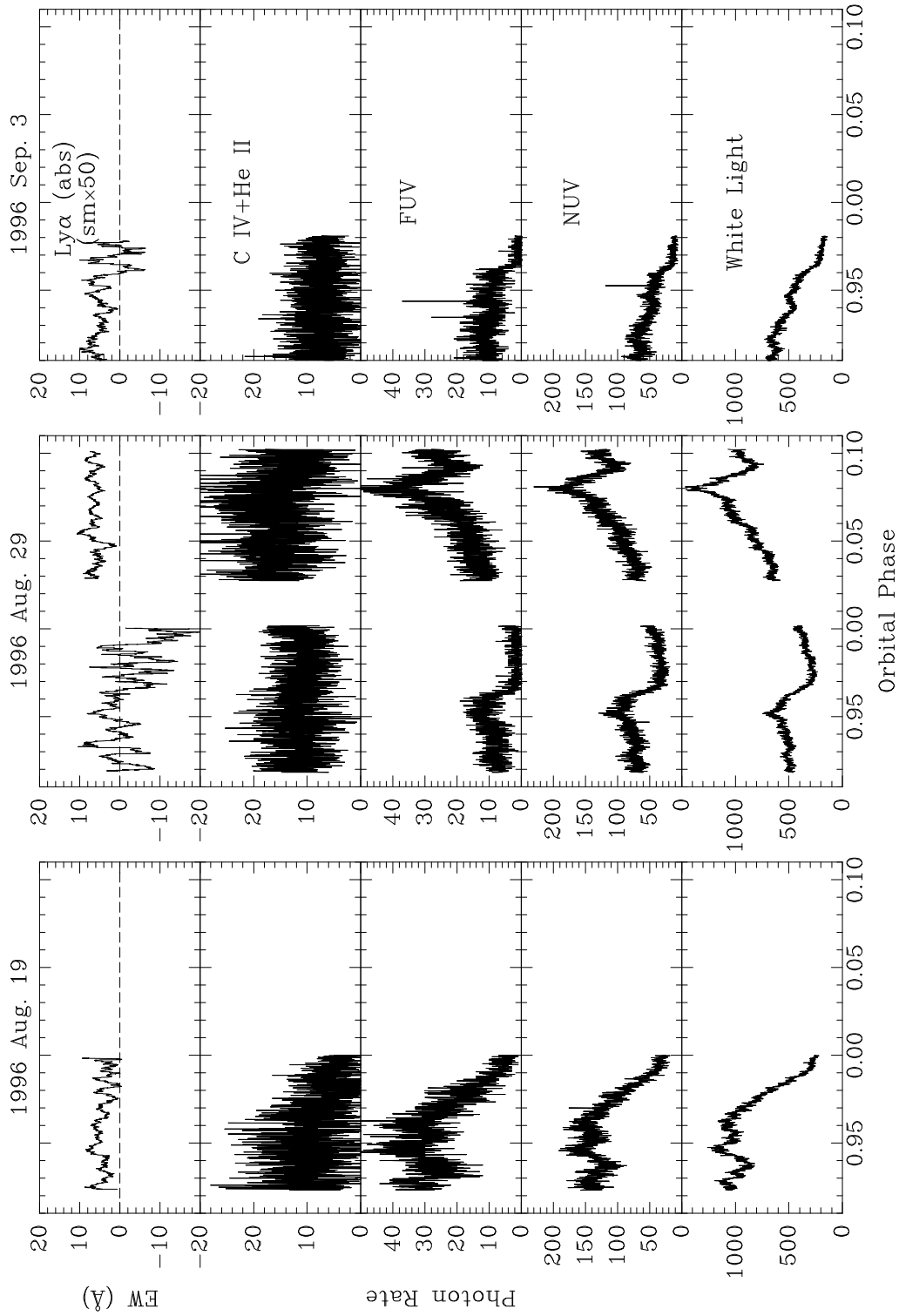


FIG. 4.— *HST* eclipse light curves for 3 epochs of the asynchronous system V1432 Aql. Included as a top series of panels is the equivalent width of  $\text{Ly}\alpha$ , smoothed over 50 time samples (40 s or  $\Delta\phi = 0.003$ ).  $\text{EW} > 0$  indicates absorption.

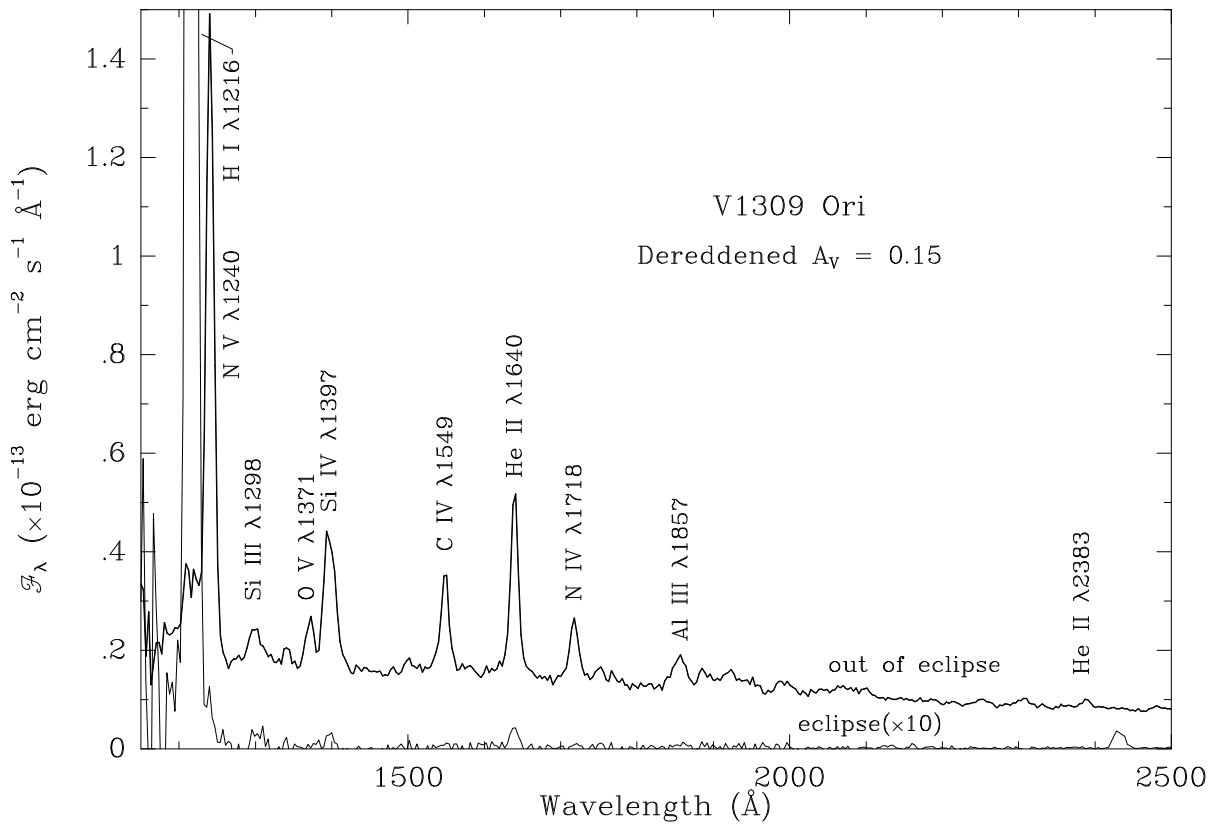


FIG. 5.— Mean in- and out-of-eclipse spectra for V1309 Ori, corrected for interstellar extinction in the amount  $A_V = 0.15$  mag. Note the unusual strength of N V  $\lambda 1240$  and N IV  $\lambda 1718$ .

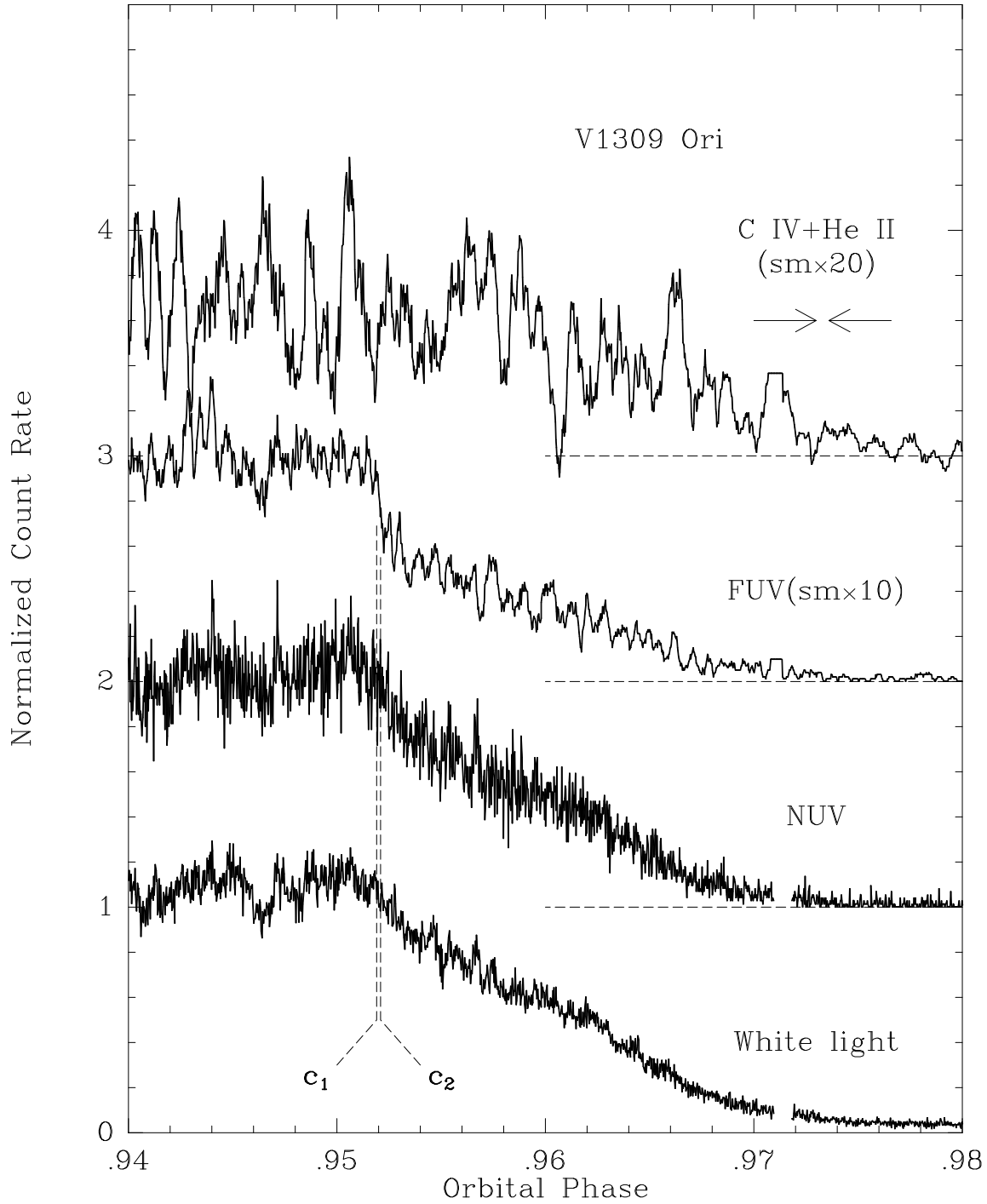


FIG. 6.— Eclipse ingress for V1309 Ori. The FUV channel has been smoothed with a running mean of width 10 time steps (8.2 s) and the emission-line band by a 20-step wide window (16.4 s or  $\Delta\varphi = 0.0006$ ). The width of the latter window is indicated by the gap between opposing arrows. Eclipse contacts  $c_1$ ,  $c_2$  in the FUV channel indicate ingress of a hot accretion spot which is unresolved in the smoothed data.

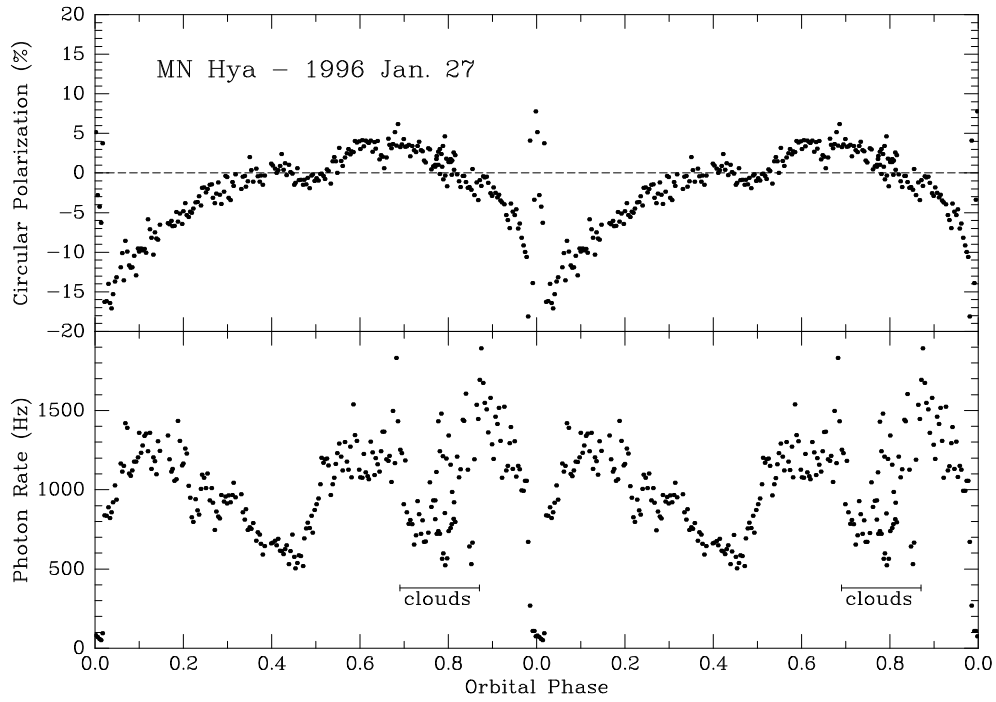


FIG. 7.— Circular polarization and brightness in the optical covering one orbital cycle of MN Hya. Note the deep eclipse at  $\varphi = 0$  and the *S*-wave in circular polarization around  $\varphi = 0.5$  associated with the two poles rotating over the stellar limb. The data are plotted twice for clarity.

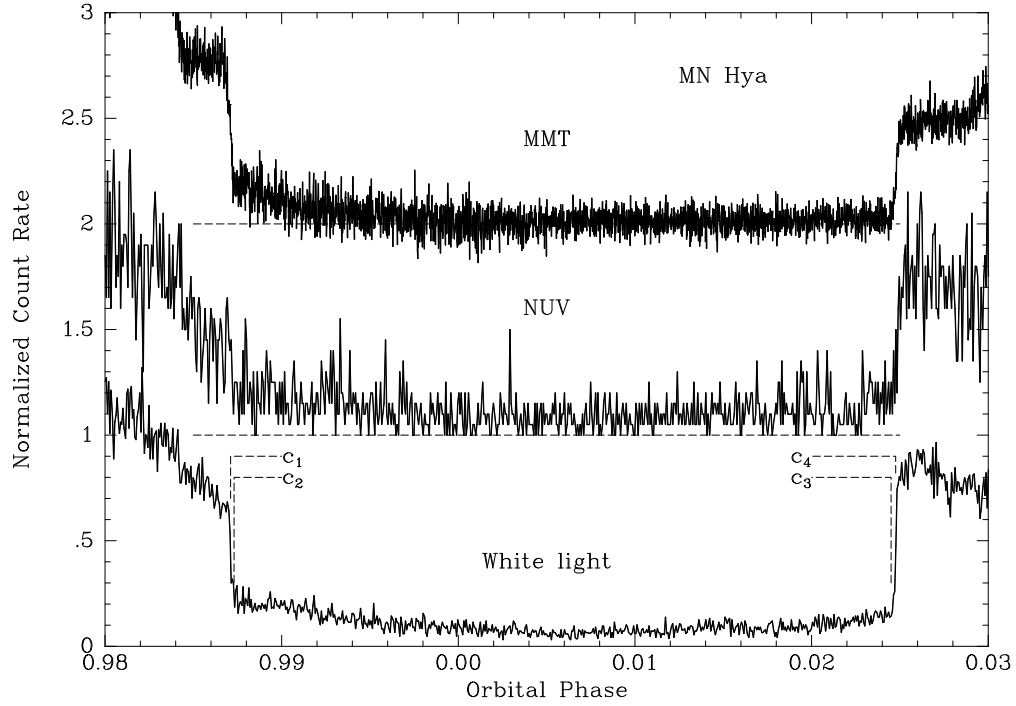


FIG. 8.— Eclipse detail of MN Hya. The top light curve is an optical light curve ( $\lambda\lambda 3500 - 6500$ ) taken on 1996 Mar. 10 at the MMT with a CCD clocked in a programmed-readout mode. Contacts mark the ingress and egress of an optical-near UV-emitting spot assigned to cyclotron emission from the accretion shock.

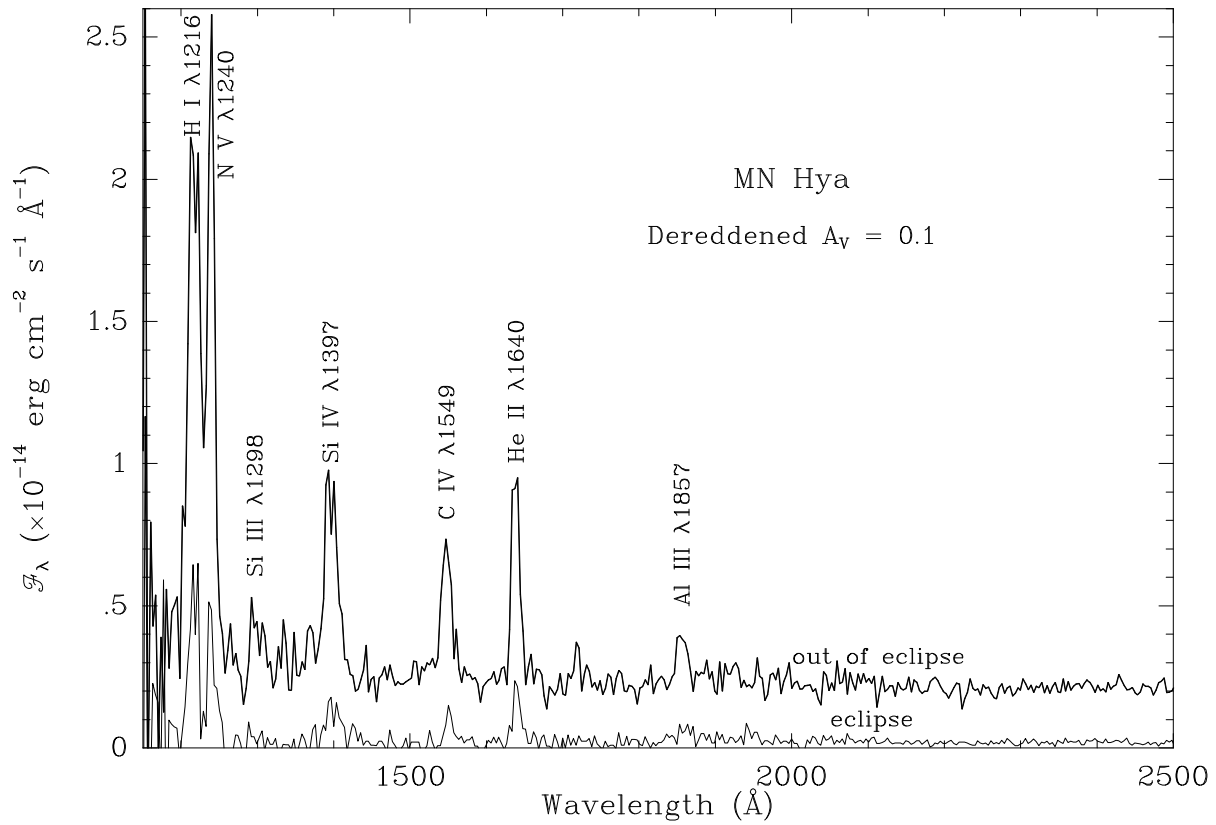


FIG. 9.— Dereddened in- and out-of-eclipse spectra of MN Hya. As for V1309 Ori, N V  $\lambda 1240$  is unusually strong and N IV  $\lambda 1718$  is probably present.

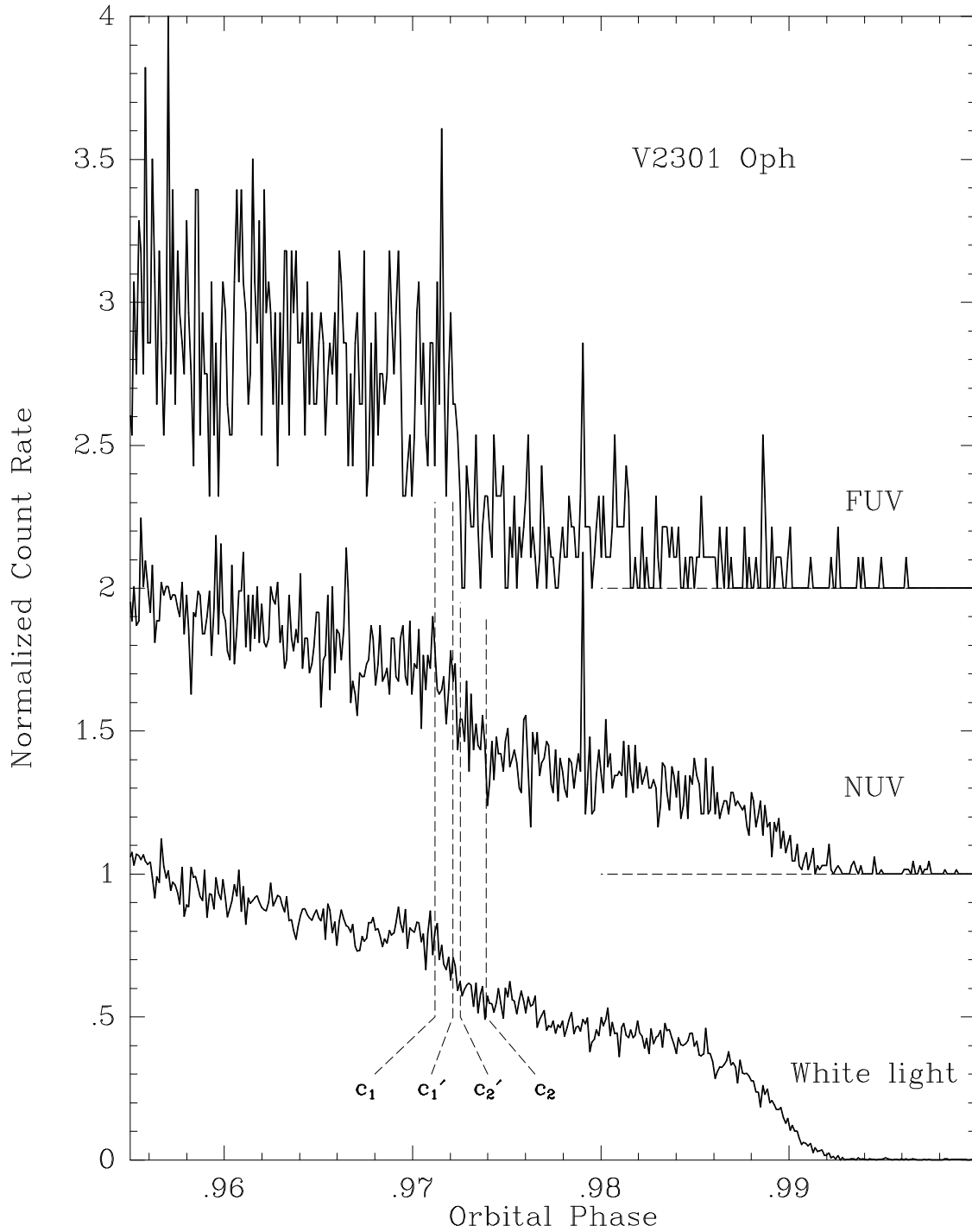


FIG. 10.— Eclipse ingress of V2301 Oph. Two pairs of ingress contacts are indicated by the data:  $c_1, c_2$  in the NUV channel, suggesting a structure approximately the size of the white dwarf, and  $c_1', c_2'$  in the FUV, which is evidence for an accretion-heated spot on the white dwarf of linear dimension  $\sim 1.4 \times 10^8$  cm and  $f_{\text{spot}} \sim 0.008$ . The extended decline to minimum light in all bands corresponds to the eclipse of the portion of the accretion stream which overshoots in azimuth the white dwarf.

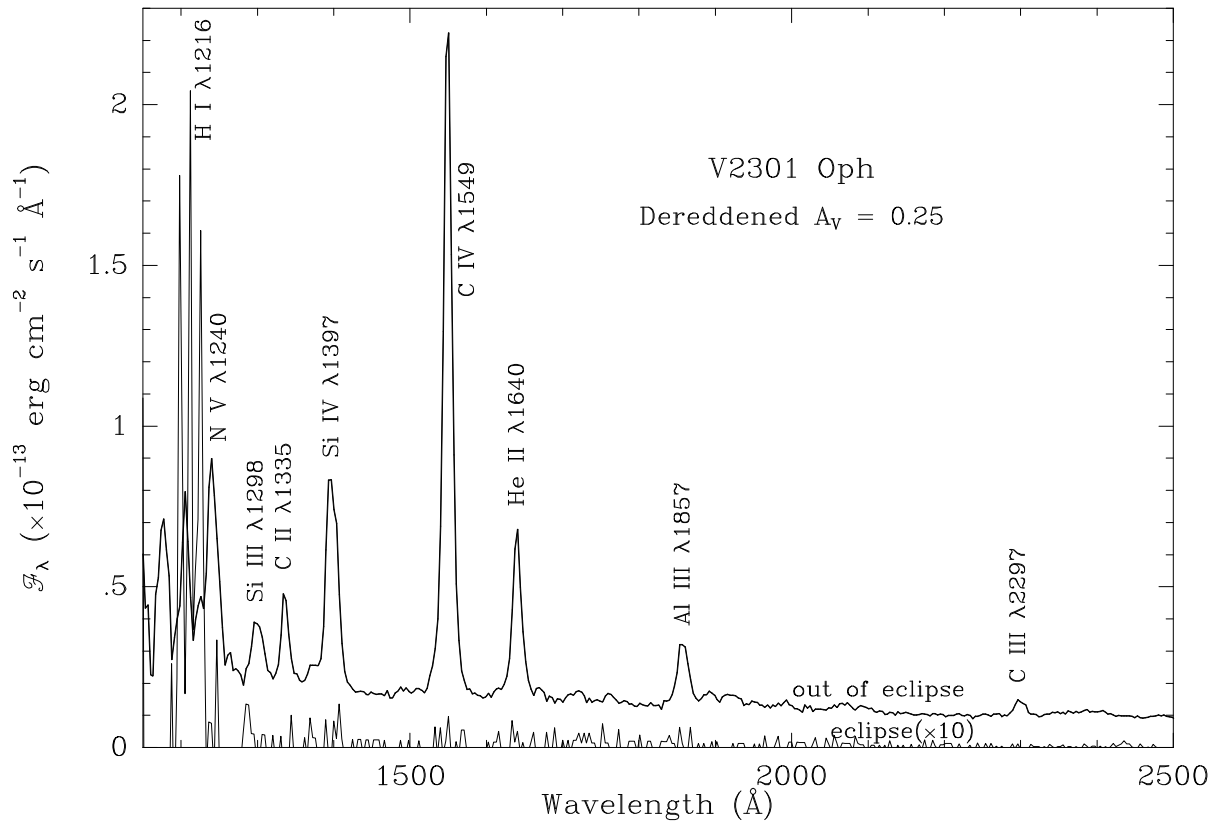


FIG. 11.— Dereddened in- and out-of-eclipse spectra of V2301 Oph.



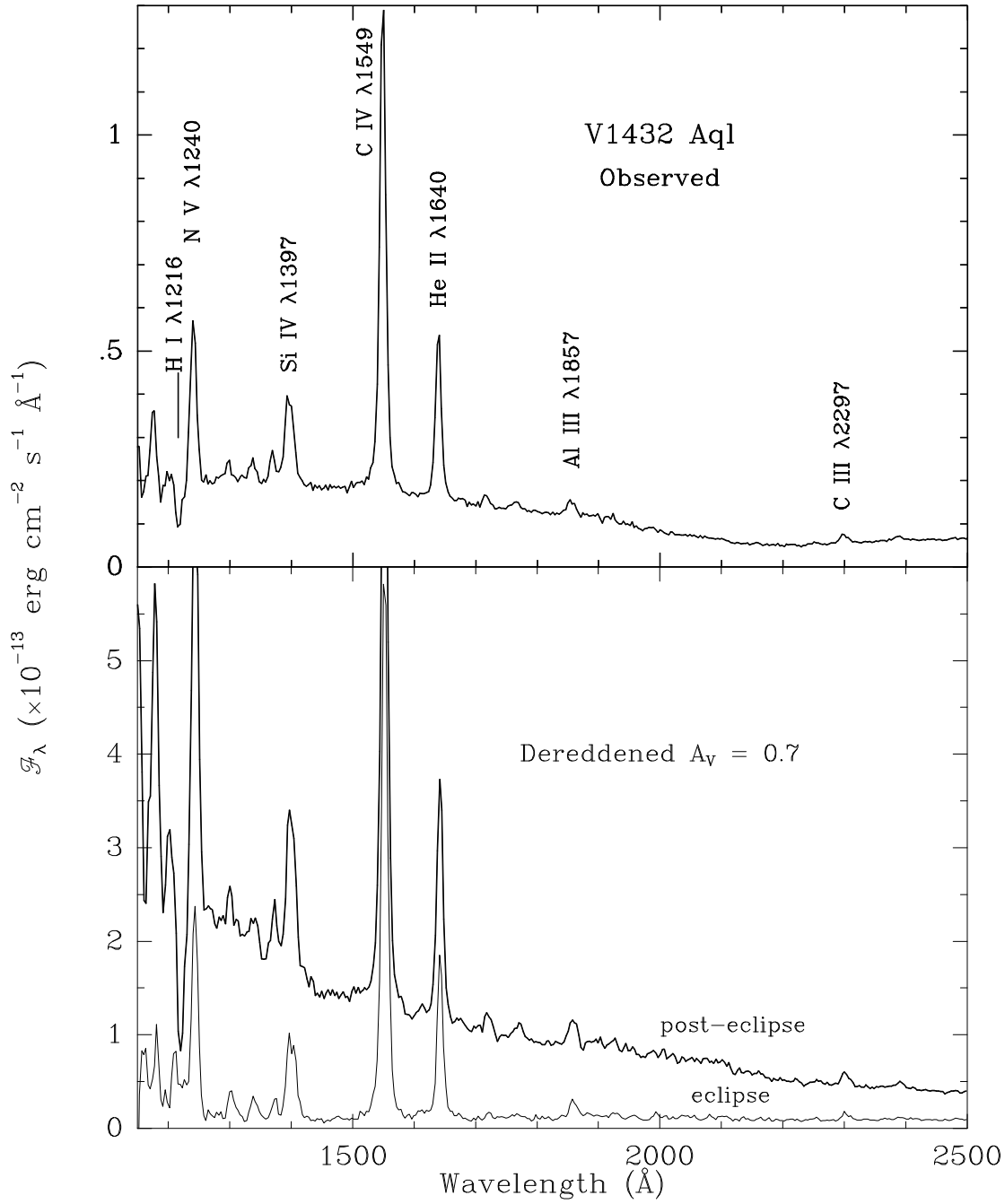


FIG. 12.— FOS spectra of V1432 Aql. (*Top*): The mean spectrum over all epochs, as observed. (*Bottom*): Eclipse and post-eclipse spectra taken from the datasets of 1996 Aug. 29, corrected for an interstellar extinction of  $A_v = 0.7$  mag. Note the steep continuum out of eclipse.